ELECTRIC VEHICLES IN A DISTRIBUTED AND INTEGRATED MARKET USING SUSTAINABLE ENERGY AND OPEN NETWORKS

WP 1.5 BATTERY MODELING

Type:	Deliverable
Identifier:	D1.5.1
Classification:	External report
Version:	1.1
Editors:	Søren Højgaard Jensen, Claus Nygaard Rasmussen, Guangya Yang (DTU)
Date:	06/01/2012

1 EXECUTIVE SUMMARY

Range has been the Achilles heel of EVs compared to cars with internal combustion engines for the last century. The properties of the electrochemical energy storage medium also known as the battery decides how much energy can be stored and subsequently transformed into propulsion. Development of the lithium ion and lithium polymer battery families has shown significant improvement in gravimetric and volumetric energy capacity during the last 20 years. Based on the current market situation and estimated utilisation areas for different chemistries the EDISON project chose to purchase Li-ion manganese spinel and lithium iron phosphate batteries for laboratory studies. Later in this chapter more information about battery module tests can be found. Information on tests on EV sized battery packs can be found in the chapter from WP6A. During the project period comprehensive research programs on battery technology have been established e.g. the ARPA-E managed by department of energy in the USA[i]. Some of the envisioned products promise an increase in gravimetric energy capacity with factor of 2-4. . Tejs Vegge, DTU is currently heading a research project funded by DSF about the very promising Li-air technology.

In WP 1.5 a simulation-model was developed in order to evaluate the effects that use-pattern has on EV battery degradation and lifetime. From a user perspective, the important parameters relating to an EV battery is energy capacity, efficiency and remaining lifetime. These parameters are strongly dependent on a number of variables such as temperature, depth-of-discharge (DOD), charge and discharge rates and cycle number. This means that battery use affects battery performance. The following aging effects are taken into consideration in the model: Depth of discharge (DOD), number of cycles, state of charge (SOC), C-rate, temperature, temperature cycling and calendar life. Figure 1 show the structure of the model.

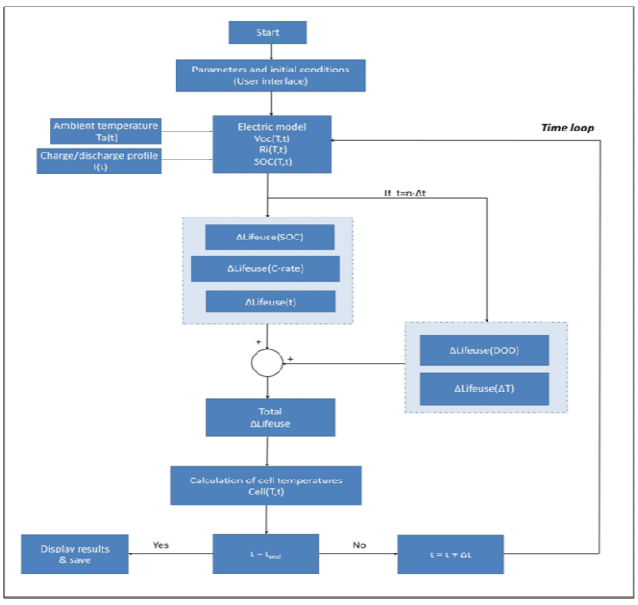

Figure 1. Sketch of the structure of the battery simulation model developed in WP 1.5.

A battery module test setup was developed at Risø DTU, ABF in order to test a 75 Ah 8-cell NMC Kokam battery module and a 50 Ah 10-cell LFP Byd battery module. Results from the battery module tests were used as input for the battery model. The setup was used to measure

the module impedance as well as the impedance of the individual cells in the module. It was observed that when a cell in a module collapses and the cell voltage drops to 0V due to harsh or prolonged operation of the module, the impedance of the collapsed cell increases dramatically. This means that even though such a cell collapse will have limited impact on the electrical performance of the EV battery pack, local heating of the collapsed cell during pack operation may lead to overheating and subsequent violent collapses of the adjacent cells. This potential safety hazard must be addressed and properly handled by the battery pack BMS system.

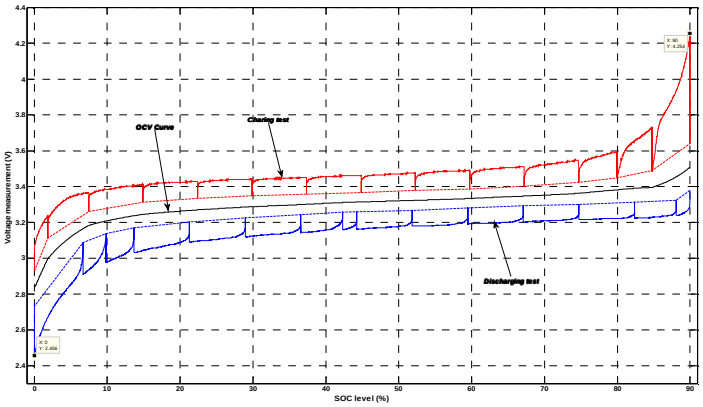

Figure 2. Measurements of the battery open circuit voltage as a function of state of charge in a LFP cell.

Further in WP 1.5, an equivalent circuit (EC) model describing the dynamic behaviour of the batteries during operation was developed. The EC model can be represented as a set of ordinary differential equations and offers a good compromise between accuracy and simulation speed. In relation to the development of the EC model, a technique to find the open circuit voltage (OCV) as a function of state of charge (SOC) was developed and applied to the batteries as seen in Figure 2. The EC model combines the OCV vs. SOC data with SOH data and measurements of the battery impedance to provide real-time information about the battery voltage and SOC as a function of the battery use. A literature study was also conducted in the Edison WP 1.5 to ensure the relevant public knowledge was present in order to accomplish the tasks executed in the WP. The Edison WP 1.5 work is described in further detail in “Batteries – methods, measurements and modeling” (see references below).

2 CONTENT OF THE EDISON WP 1.5 FINAL REPORT

3 PURPOSE OF WP 1.5

The purpose of WP 1.5 is to construct a model that describes battery degradation and the battery state of health (SOH) as a function of battery use and to construct a model that describes the dynamic behavior of battery modules as a function of battery use. The objective is to gain knowledge about the overall performance of the batteries as function of different charging/discharging patterns and different battery types for future EV's. Two battery chemistries were tested in order to obtain data for the models: Lithium-nickel-manganese-cobalt-oxide (NMC) batteries and Lithium-Iron-Phosphate (LFP) batteries.

The battery models give detailed information about different chemistry's abilities. This information includes:

- The charge voltage/current profiles and discharge voltage/current profiles as a function of state-of-charge for the different chemistries.
- The effect of different charging/discharging patterns to the cycle life time and performance of the batteries

The battery models contain the technical data needed to program appropriate battery system models of EV's for use in a power system analysis tool, i.e. aggregated models dealing with overall parameters like charging/discharging pattern, battery degradation, battery system loss etc.

3.1 CONNECTION TO OTHER WP'S

WP 1.5 is connected to several other work packages in the Edison project. Here a short overview of the connection to other work packages.

3.1.1 WP 2.2

WP 2.2 needs a battery model that can model the behavior of the battery when utilized for grid purposes. Thus it must model the available capacity and V,I characteristic of the battery considering aging and temperature. Especially the aging of the battery due to cycling and fast charging should be represented by the model.

3.1.2 WP 3

WP 3 needs a battery model that can be implemented for the purpose of examining the communication interface. It is therefore important that the battery model captures the essentials of the battery behavior. The requirements for the model should be determined by WP 2.2 and WP 4.

3.1.3 WP 4

WP 4 needs a battery degradation model, that is valid and reliable also under fast charging conditions (i.e. high current and high temperature), to optimise the fast charging algorithm. WP 4 (+ WP 6a) will test the battery degradations for different fast charging algorithms. The results may be used to verify and calibrate the battery degradation model.

3.1.4 WP 6A

Different load patterns (including normal charging, fast charging and normal driving loads) will be applied to both types of battery packs, and the battery performance parameters (i.e. the energy capacities and the energy losses) will be checked on regular basis. The results may be used to verify and calibrate the battery degradation model.

4 BATTERY TESTING

As mentioned above, two battery chemistries were tested, namely a 75 Ah NMC module from KOKAM and a 50 Ah LFP module from BYD. Batteries were tested both at Risø DTU, ABF and at DTU Electro. Here we describe some of the test results and the measurement methods used to characterize the battery modules.

Section 4.1 is devoted to a description of the test methods used to characterize the battery modules tested at Risø DTU. Section 4.2 describes some of the test results obtained at Risø DTU, ABF and Section 4.3 describes some of the test results obtained at DTU Electro. The test results were used as experimental input for the models described in Section 5.

4.1 CHARACTERIZATION OF A NMC LITHIUM BATTERY MODULE

Before the degradation tests the two battery modules were characterized both with charge discharge cycles at several temperatures (typically 0 ^{o}C, 23 ^{o}C and 50 ^{o}C) and impedance spectra measured at various state of charge (typically 25% SOC, 50% SOC and 90% SOC) and temperature (typically 0 ^{o}C, 23 ^{o}C and 50 ^{o}C). Here we give a detailed description of the characterisation method and some of the characterisation measurements on the NMC battery module. The data was used in the models described in section 5.

4.1.1 ABSTRACT

Detailed characterisation of battery modules is necessary to construct reliable models that incorporate performance related aspects of the modules such as thermodynamics, electrochemical reaction kinetics and degradation mechanisms. Charge-discharge curves, temperature and battery impedance measurements can provide detailed information about these aspects. Charge-discharge curves can be used to measure the battery open circuit voltage and the internal resistance. Temperature measurements provide information about the thermodynamic reactions and impedance spectra yield detailed information about the reaction kinetics. In this paper we present the measurement method that we use to examine the internal resistance, the capacity and the impedance of a 75 Ah NMC battery module. In order to measure the impedance of the battery module and of the individual cells in the module, we combine the single sine technique and the Laplace transformed excitation signal technique which both have pros and cons. By combining the two impedance measurement techniques we are able to reduce the measurement time by a factor of 20.

4.1.2 INTRODUCTION

During the last decade a rapidly increasing interest in batteries for propulsion in the transport sector has emerged. Since battery performance is drastically affected by the operation pattern it is important to quantify the battery degradation as a function of the operation pattern. This is not a trivial task since the battery performance is not a measurable quantity in itself, but covers several aspects such as the internal resistance of the battery and the battery capacity. Further, the operation pattern covers several aspects such as the Depth of Discharge (DOD), C-rate and temperature and calendar life.

In order to quantify the battery module wear due to specific operation patterns, we suggest to perform micro-cycle tests where a single operating parameter is varied slightly while keeping the other operating parameters as constant as possible. The internal resistance, the capacity and the impedance of the cells and the module should be measured before and after each series of micro-cycles. In this way it is possible to map the battery module wear as a function of the various operating conditions and thus to develop a model that predicts the module wear due to a more complex operating pattern as described by Safari et al. [1]. In a subsequent paper we will use the measurement method presented here to measure the NMC battery module wear before and after such micro-cycle tests. Here we describe the details of the measurement method.

Battery impedance spectra provide valuable knowledge about the reaction kinetics of physical/chemical processes taking place inside the battery. For this reason the impedance spectra can provide information that can be used to develop improved SOH models and to describe how the battery voltage (or current) responds to rapid changes in the current (or voltage) [2,3]. Normal single sine measurement techniques to obtain impedance spectra on batteries are very time consuming. Klots et al have recently presented a very advanced work on combined TDM and EIS measurements of a Li-ion cell with an internal resistance in the order of 0.5 Ω [4,5]. Here we also present results on combined TDM and EIS measurements, but we use the TDM method to simultaneously obtain impedance spectra on eight cells in a battery module and the cell impedances are on the order of 1 mΩ. Also, the

transformation of the TDM measurements into the frequency domain is different from that presented by Klots et al. Further, Klots et al. use a voltage step whereas we use a current step from 0 A to 1 A.

4.1.3 EXPERIMENTAL

The tested battery module is a SLPB125255255H module supplied by Kokam Co. Ltd. The module consists of eight serially connected 75 Ah cells in with lithium-nickel-manganese-cobalt-oxide cathodes and lithium-carbon anodes. The cells electrolyte consist of lithium salt e.g. LiPF6, organic solvent such as ethylene carbonate, gel polymer and performance/safety enhancing additives. The cells are usually referred to as NMC cells and Kokam supplies the following technical specification for the NMC cells: The minimum discharge cell voltage is 3.0 V, the nominal voltage is 3.7 V and the maximum charge voltage is 4.15 ± 0.03 V.

The battery module voltage, the individual cell voltages, the current and the temperature were continuously logged during the module characterization. The module charge capacity was tested with a charge-discharge curve ranging from the manufacturer's maximum charge voltage to the minimum discharge voltage. The charge-discharge cycle consists of a series of discharge steps followed by a series of charge steps. Each step lasts six minutes and consists of five minutes of either charging or discharging at 0.13 C, i.e. at either 10 A or -10 A, and one minute at 0 C i.e. at 0 A.

We define the module to be fully charged when the voltage of one of the cells in the battery module reach 4.15 V at a low C-rate. The state of charge (SOC) of the fully charged battery module is defined as 100% SOC. The fully discharged battery module, i.e. when one of the cells in the battery module reaches 3.0 V at a low C-rate, is defined as 0% SOC. SOCs between 0% and 100% are measured by subtracting the net discharge flow from the fully charged module divided with the measured module charge capacity, i.e. by Coulomb counting.

This SOC definition does not fully account for self-discharge with time and non-ideal Coulombic efficiency of the battery. The self-discharge of the module prior to any degradation tests was approximately 1 mV per day and can thus be ignored during the initial characterization. However, non-ideal Coulombic efficiency could lead to large accumulated errors in the Coulomb counting SOC measurement, especially when the battery is cycled several times without reaching fully charged or discharged condition where it is possible to re-calibrate the SOC. For this reason we suggest to use the battery open circuit voltage (OCV) to re-calibrate the SOC whenever the battery has been at rest for 1 hour. In order to measure the module OCV as a function of SOC we use a method previously described by Shark and Doerffel who used it for fast OCV measurements at high C-rates [6]. The voltage measurement during the 0 C periods in the charge-discharge steps described above is used to determine the OCV vs. SOC. This is described in further detail with the presentation of the measurements in the result section.

The module and cell impedances were measured with normal single-sine impedance spectroscopy using a Solartron 1252A. A Kepco BOP 50-4M was used to boost the 16 mA AC current from the Solartron to 1 Ampere AC. The coax-cables from the solartron to the individual cell-electrodes are multiplexed with a Keithley 2750 and three Keithley 7700 cards to enable automated measurements without having to move the impedance cables. All temperatures were logged with a Keithley 7702 card. The module and cell impedance was also measured with a Laplace transform of the module and cell over-voltage. The over-voltages were measured as a function of time after onset of a step-current of 1 Ampere. The data acquisition lasted one hour and the data was measured every 2nd second.

4.1.4 RESULTS

The battery module temperature and voltage were measured as a function of time during a full charge-discharge cycle, see Figure 3. Before the charge-discharge cycle, the module was charged to 100% SOC. This was done in steps of 6 minutes. In each step, the battery was first charged with -10 A for five minutes, and the current was reduced to 0A for one minute. As soon as one of the eight cells in the module reached the maximum charge voltage of 4.15 V, the current was interrupted and the current state of charge was defined as 100% SOC.

Immediately after this, the module was discharged with 10 A for 5 minutes. Then the battery current was set to 0 A for one minute. This was repeated until the one of the eight cells in the module reached 3 V. After this, the module was charged in steps of 5 minutes with -10 A and 1 minute at 0 A until one of the eight cells reached 4.15 V (100 % SOC).

The battery capacity was measured as the current multiplied with the total time during discharging. The battery capacity was found to be 75.3 Ah when the ambient temperature was 22 ^{o}C. The initial temperature of the battery module is higher than the ambient temperature due to pre-charging to reach 100% SOC. Note how the battery heats up during the first three hours of discharging and cools down subsequently. This is thought to be due to entropy changes arising from structural transformations in the Li-C anode and NMC cathode phase changes [7-10].

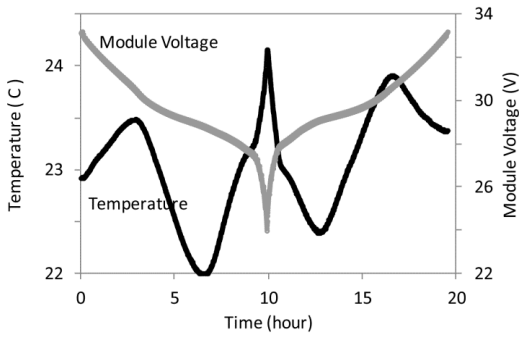

Figure 3. Voltage and temperature measured as a function of time during a charge-discharge cycle of a 75 Ah NMC battery module.

The module voltage as a function of state of charge is shown in Figure 4. The grey line shows the module voltage during the 5 minute-periods at 0.13 C. The black points in the figure show the module voltage just before the end of the 1 minute-periods at 0 C. As described by Abu-Sharkh and Doerffel [6] an estimate of the OCV at a given SOC can be obtained as the average voltage of the upper and lower black points. If the periods at 0 C had been sufficiently long, the module voltage would relax until it reaches OCV. The black line in Figure 4 show this calculated OCV estimation.

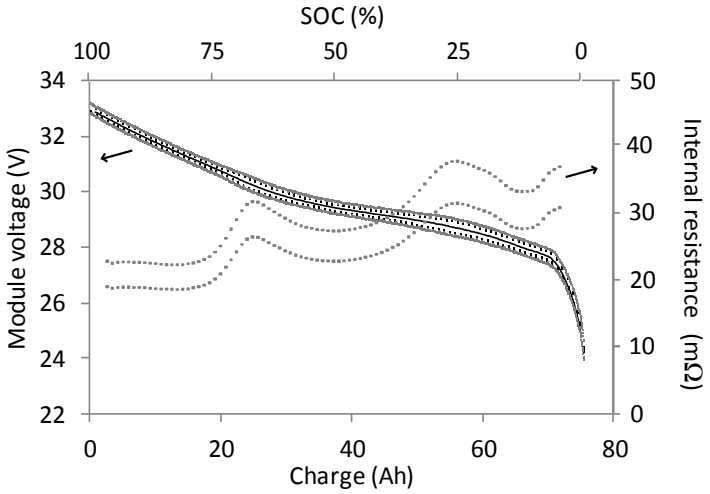

Figure 4. Charge-discharge curve for the 75 Ah NMC battery module. The charge-discharge curve is made as a series of discharge steps followed by a series of charge steps. Each step takes 6 minutes: 5 minutes at 0.13 C and one minute at 0 C. The grey line show the module voltage during 0.13 C. The black points show the module voltage during 0 C. The black line shows the SOC calculated from the black points. The grey points show the upper and lower estimate of the internal resistance derived from the difference between the upper and lower grey curve.

The internal resistance of the battery module as a function of SOC can be estimated as the difference between the upper and lower grey curve in Figure 4 divided by the difference between the charge and discharge current. However in this calculation, it is unclear whether we should use the discharge current during the periods of discharging, i.e. 10 A or use the average discharge current, i.e 10 A · 5 min/ 6 min = 8.3 A? Likewise, different values will be calculated using -8.3 A or -10 A as the charge current, but it is not certain which is more accurate. This is not a trivial question to answer since the very slow electrochemical processes in the battery module with a characteristic time much larger than 6 minutes will respond to the average charge/discharge current whereas the fast processes with a characteristic time of less than 5 minutes will respond to the actual charge/discharge current. For this reason it requires a detailed analysis of the module and cell impedance spectra to give a precise estimate of the internal resistance. This is beyond the scope of this article and instead we will use the average and actual charge/discharge current to give an upper and lower estimate of the internal resistance of the module as a function of SOC. This is shown as the grey points in Figure 4. Note that the gap between the upper and lower estimate can be reduced or even removed by decreasing the number of – or completely omitting - the 1 minute waiting periods at 0 C.

The module impedance was measured at 90% SOC. This was done both in an ordinary single-sine measurement with a Solartron 1252A and with a Laplace transformed over-voltage curve. The over-voltage as a function of time after onset of a step-current of -1 Ampere is shown in Figure 5. The over-voltage is measured approximately every 2nd second for one hour.

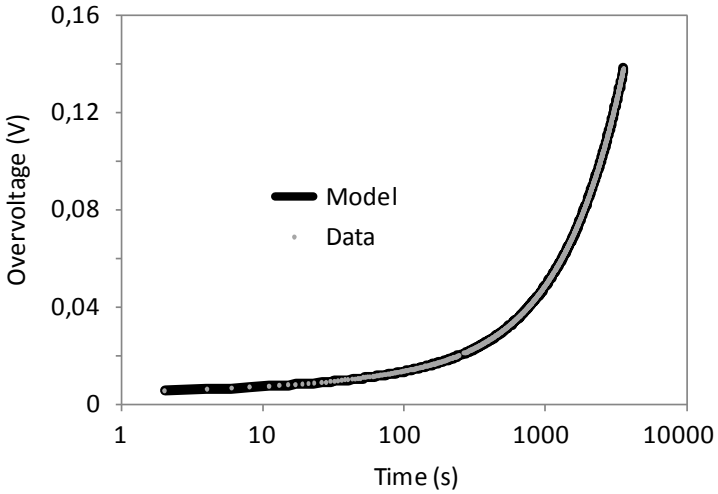

Figure 5. Overvoltage measured on a 75 Ah NMC battery module as a function of time after onset of -1 A current. The grey dots are the measured data. The black line is a model of the overvoltage. We use the model to derive the low frequency impedance of the battery module.

We have chosen to model the overvoltage in Figure 5 as follows. The current in the time domain can be written as $I(t) = I_0 \cdot u(t)$ where I_0 is the current amplitude, i.e. -1 Ampere and u(t) is a step function which is 0 when $t < 0$ and 1

when t ≥ 0. The Laplace transform of I(t) is I(s) = I_0/s, where s = jω, j is the complex unity and ω is the angular frequency. $R_sC_{bat}(RC)_1(RC)_2(RC)_3$ is an equivalent circuit where R is a resistor and C is a capacitor and (RC) is a parallel connection between a resistor and a capacitor.

The overvoltage in the frequency domain (or s-domain), U(s) is the product of I(s) and the impedance of the equivalent circuit, i.e.

$$U(s) = \frac{I_0}{s} \cdot \left(R_s + \frac{1}{sC_{bat}} + \frac{R_1}{1+sR_1C_1} + \frac{R_2}{1+sR_2C_2} + \frac{R_3}{1+sR_3C_3} \right)$$

The overvoltage in the time domain, U(t) is given as the inverse Laplace transform of $U(s)$:

$$U(t) = u(t) \cdot I_0 \left[R_s + t \cdot C_{bat} + R_1 \left(1 - e^{\frac{-t}{R_1C_1}} \right) + R_2 \left(1 - e^{\frac{-t}{R_2C_2}} \right) + R_3 \left(1 - e^{\frac{-t}{R_3C_3}} \right) \right]$$

In order to fit the model of U(t) to the overvoltage curve, R_s was fixed at 5.7 mΩ, the value of the real part of the impedance measured with the single-sine measurement method at 0.3 Hz. R_s was fixed in order to assure a stable conversion of the fitting routine. The remaining variables in the circuit were obtained by fitting the model to the data in Figure 5. The R- and C-values obtained from the fit were used to calculate the model impedance. The model impedance is shown in Figure 6 together with the battery module impedance measured with the single-sine measurement method. From the figure it is seen that the two methods yields reasonably accurate data below 60 mHz. Above 60 mHz the laplace method measurements (not shown) increasingly deviate from the single-sine measurements due to the limited data acquisition frequency and due to a non-optimized model for the battery impedance.

In order to measure the changes in the electrode kinetics of the individual cells of the module, we measured impedance spectra on the individual cells in the battery module. Just as we did with the measurements of the battery module impedance spectra shown in Figure 6, the spectra were measured both with the single sine measurement method and with the TDM measurement method. Again, in order to fit the model to the spectra, R_s was fixed at 0.73 mΩ, the value of the real part of the impedance measured with the single-sine measurement method at 0.3 Hz. Again, R_s was fixed in order to assure a stable conversion of the fitting routine.

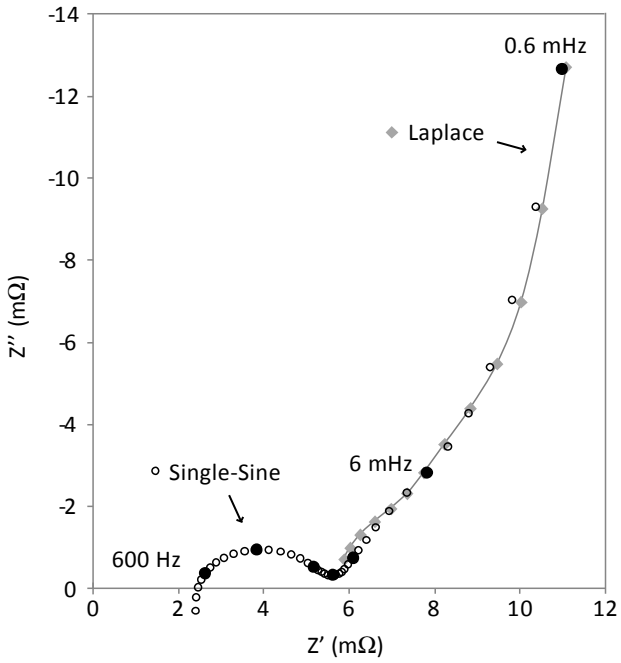

Figure 6. Impedance measured on the 75 Ah NMC module. The Impedance is measured both with a Single-Sine method and a Laplace method. The Single-Sine measurements shown with black markers denote the frequency decades. The two methods overlap reasonably well below 60 mHz. The Single-Sine method is the most accurate method at high frequency but it can take a very long time for measurements at low frequencies. This makes it interesting to combine the two methods.

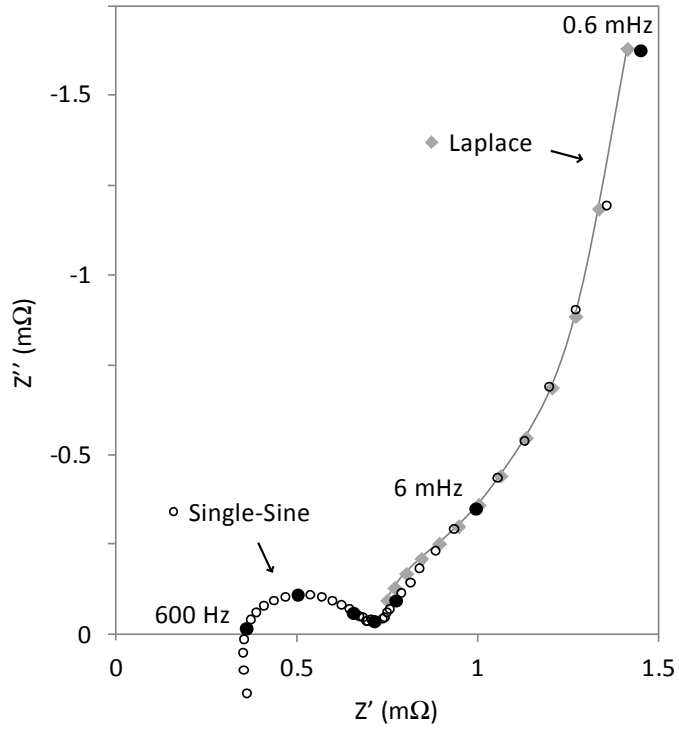

Figure 7. Impedance measured on a single cell in the 75 Ah NMC module. The Impedance is measured both with a Single-Sine method and a Laplace method. The Single-Sine measurements shown with black markers denote the frequency decades. The two methods overlap reasonably well below 60 mHz.

It should be noted that the battery overvoltage U(t) can be predicted by the inverse Laplace transform of U(s). In order to obtain U(s) it is necessary to establish a simple model of the battery impedance, e.g. as the impedance of an equivalent circuit $R(RC)_1(RC)_2\ldots(RC)_n$. A sufficient number of (RC) circuits should be chosen to assure a good fit between the measured impedance and the impedance of the model. U(s) is the product of the model impedance and I(s), the Laplace transform of the current I(t).

4.1.5 DISCUSSION

The data in Figure 3 provides interesting information about the thermal behavior and the voltage of the NMC battery module during charging and discharging. As previously noted, the change in exothermal/endothermal behavior of the battery module is thought to be due to entropy changes arising from structural transformations in the Li-C anode and NMC cathode phase changes [7-10] which in turn leads to the observed changes the temperature inside the battery module. The module voltage presented in Figure 3 was used to derive the internal

resistance of the battery module as shown in Figure 4. Here two local maxima for the internal resistance are observed. One at about 25% SOC and one at about 75% SOC. By comparison with Figure 3, it is seen that the maximum in the internal resistance at app. 25% SOC occurs when the battery module temperature reaches a local minimum. Such a temperature dependence of the internal resistance is also expected and can be explained by the thermally activated electrode reactions [9]. However, the local maxium of the internal resistance at app 75% SOC occurs when the battery temperature reaches a local maximum. The reason for this local maximum in the internal resistance is currently not fully understood by the authors.

In Figure 4 the resistance was measured after 5 minutes (the grey dots) of constant current operation. At 90% SOC, the measured resistance was 18 - 22 mΩ. The real part of the impedance at 0.6 mHz is 11mHz. The reason for this difference is due to the very slow processes in the battery that are affected on time-scales greater than 1/0.6 mHz = 28 minutes. Further, the ambient temperature during the measurement in Figure 6 was 24 ^{o}C whereas it was 22 ^{o}C during the measurement in Figure 4. This may also explain some of the deviation between the two resistance measurements.

The Single-Sine method is the most accurate method at high frequency but the method can also results in long measurement times at low frequencies. It can only be used on a single cell or on the module at a time. The Laplace technique can be used to obtain impedance information on all eight cells and on the battery module at the same time. Further, the Laplace technique yields information about the impedance at all frequencies above a f_{min}=1/sampling time (in our case f_{min} = 1/3600 s) whereas the single-sine measurement technique only provides information of the impedance at a single frequency and hence each data points needs to be measured sequentially. As an example, with the single sine-measurement technique it takes approximately 30 hours to measure impedance spectra on 8 cells plus the module down to 0.6 mHz. With the Laplace technique it only takes one hour. The remaining data from 60 mHz to 2610 Hz measured with the single sine method on 8 cells plus the module takes less than 30 minutes. For this reason a much faster data acquisition can be obtained together with a good precision in the entire frequency range when the two measurement techniques are combined. In the current example it is possible to reduce the data acquisition time with a factor of 20.

4.1.6 CONCLUSION

The voltage and temperature were measured during a full charge-discharge cycle on a 75 Ah NMC battery module supplied from KOKAM. The module temperature exhibited a complex behavior during the charge-discharge cycle which is most likely due to the structural transformations and phase changes in the battery electrodes during the changes in the state of charge of the electrodes. The internal resistance of the module was derived from the voltage measured during the charge-discharge cycle. The internal resistance exhibits two local maxima at app. 25%

SOC and 75% SOC. The local maximum of the internal resistance at 25% SOC correlates with a local minimum of the battery module temperature. This can be explained by the thermally activated electrochemical reactions in the battery electrodes. The local maximum of the resistance at 75% SOC occurs at a local maximum of the module temperature and is not fully understood.

The battery module impedance as well as the impedance of a single cell in the module were measured both with single sine measurements and with a Laplace transformed step-current voltage response, referred to as a time domain measurement (TDM). The two techniques show good correlation at frequencies below 66 mHz, but deviate at higher frequencies. The TDM measurements can be conducted simultaneously on both the battery module and all the cells in the module whereas the single sine measurement technique is conducted on either the module or one of the cells at a time. For this reason it is possible to reduce the impedance measurement time on the NMC module and all its cells by a factor of 20 without losing too much of the measurement accuracy.

4.1.7 REFERENCES

[1] M. Safari, M. Morcrette, C. Delacourt, M. Safari and A. Teyssot, *J. Electrochem. Soc.*, **157**, A892-A898 (2010).

[2] K. Müller, D. Tittel and P. Büschel, in *The 25th World Battery, Hybrid and Fuel Cell Electric Vehicle Symposium & Exhibition*, 25 Shenzhen, China (2010).

[3] O. Tremblay and L. Dessaint, in *The 24th World Battery, Hybrid and Fuel Cell Electric Vehicle Symposium & Exhibition*, 24 Stavanger, Norway (2009).

[4] D. Klotz, M. Scho¦ênleber, J. P. Schmidt, E. Ivers-Tiffe¦üe and E. Ivers-Tiffe¦üe, *Electrochim Acta*, **56**, 8763 (2011).

[5] D. Klotz, M. Schönleber, J. P. Schmidt and E. Ivers-Tiffee, p. s06-P-011, International Society of Electrochemistry, (2011).

[6] S. Abu-Sharkh and D. Doerffel, *J. Power Sources*, **130**, 266 (2004).

[7] R. E. Williford, V. V. Viswanathan and J. G. Zhang, *J. Power Sources*, **189**, 101 (2009).

[8] S. Al Hallaj, R. Venkatachalapathy, J. Prakash and J. R. Selman, *J. Electrochem. Soc.*, **147**, 2432 (2000).

[9] S. Noboru, *J. Power Sources*, **99**, 70 (2001).

[10] S. Al Hallaj, J. Prakash and J. R. Selman, *J. Power Sources*, **87**, 186 (2000).

4.2 DEGRADATION TESTS OF BATTERY MODULES

The aim of the work in WP 1.5 was to characterize the NMC and LFP battery modules. This can be accomplished by a series of micro cycle tests. A micro cycle test is a test where one of the operating parameters of the battery module is slightly varied while all other operating parameters is kept as constant as possible. By measurements of the change in the charge capacity, internal resistance and impedance of the battery modules due to the micro cycle tests it is possible to identify operating conditions that severely wear the battery modules. Further, it is possible to use the micro cycles to create a model that predicts the battery wear as a function battery usage history as described by Safari et al. [1]. An example of a micro cycle test is shown in Figure 8. We ran 238 of these micro cycles at 40 °C, 50 Ampere on the NMC battery module.

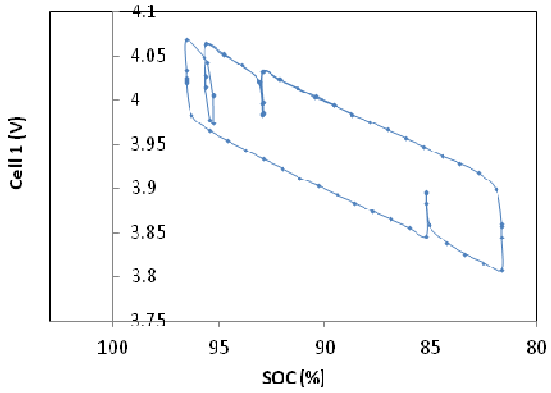

Figure 8. Micro cycle of cell 1 in a NMC battery module. 238 micro cycles was executed at 40 °C and 50 Ampere.

Charge discharge curves were measured before and after the 238 cycles. As seen from Figure 9 the charge capacity of the module has clearly decreased due to the micro cycling. The internal resistance is also seen to increase due to the 238 micro cycles, since the voltage difference between the charge voltage and discharge voltage at a given SOC is larger after the cycles than before the cycles. The internal resistance can be measured as the the voltage difference between the charge voltage and discharge voltage at a given SOC, divided with the current difference between the charge current and the discharge current as explained in relation to Figure 4.

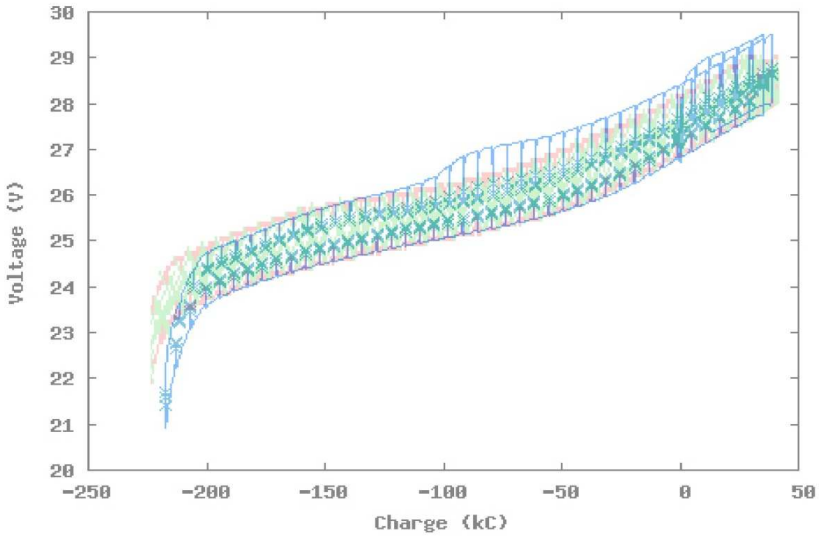

Figure 9. Charge discharge curves on the NMC battery module before and after 238 micro cycles as shown in Figure 8. The red/green curve shows the charge discharge curve before the micro cycle tests and the blue/purple curve shows the charge discharge curve after the micro cycle tests. Note how the battery capacity has decreased and how the internal resistance, in particular at higher SOC (high voltage) has increased.

Before we ran the 238 micro cycles on the NMC battery module it that had suffered a complete discharge. This damaged one of the cells in the module to the extent that it could not be recharged. The cell voltage of the damaged cell never increased to the nominal cell voltage after the complete discharge. Instead the cell voltage of the damaged cell kept on relaxing to 0 V shortly after the module was left at OCV. Further, the impedance of the damaged cell increased significantly which must have caused an increased heating of the damaged cell during the micro cycle tests. It was not possible to detect this local heating of the damaged cell since the battery module was only supplied with four temperature measurement probes. None of the four temperature measurements exceeded the permitted temperature during the micro cycle tests. However, as seen from Figure 10 it is obvious that the battery module is not safe to operate with one damaged cell. For this reason it is important to know the internal resistance of the individual cells in order to avoid local heating.

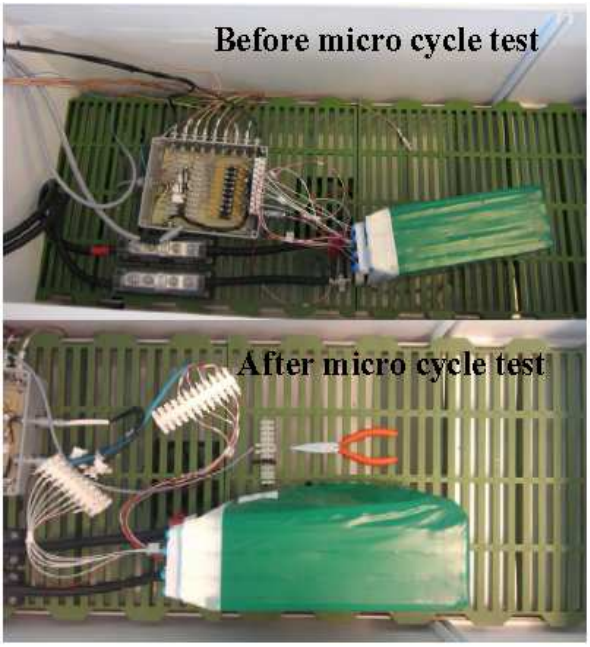

Figure 10. The NMC battery module before and after the 238 micro cycles. Note how one side of the NMC module expanded due to the micro cycle tests.

Similar micro cycle tests were applied to the LFP module. It was tested with 172 micro-cycles at 20 °C, 25 Ampere. The module was subsequently characterized with a charge-discharge cycle. Even though the operating conditions during the micro cycle was pretty mild, one of the cells in the module did not survive the charge-discharge curve. The cell voltage of the damaged cell never reached the nominal cell voltage. Instead the cell voltage of the damaged cell continuously kept relaxing to 0 V shortly after the module was left at OCV. Again, the impedance of the damaged cell increased dramatically. However, it was still possible to examine the wear on the other cells that were not damaged. As seen from the impedance spectra in Figure 11 the impedance increases during the micro cycle tests. The spectra were measured on two of the cells in the module before and after the micro cycle tests and they were measured at 23 ^{o}C at 90 SOC.

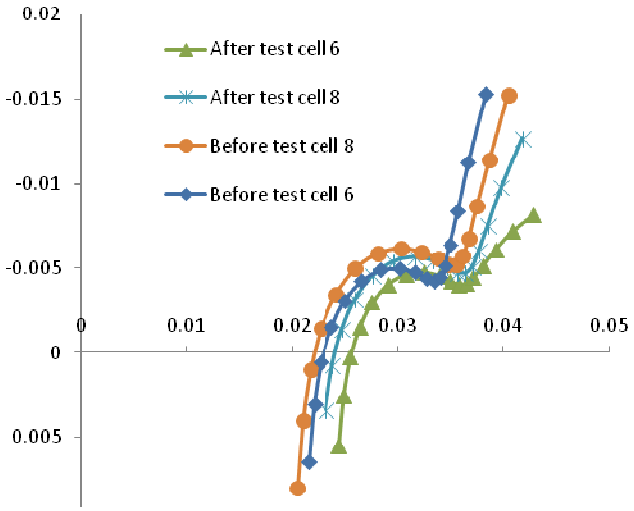

Figure 11. Impedance spectra measured on two of the cells of the BYD module before and after the 172 micro cycles. The frequency range is from 1 Hz to 400 Hz.

The data obtained from the micro cycle tests on the two battery modules was used in Section 5.1 and 5.2 to form the experimental input to construct the battery models.

4.3 BATTERY TESTING LABORATORY SETUP AND PRELIMINARY RESULT

The laboratory of a test-bench for battery testing is composed by a lithium-ion phosphate (LFP) battery pack, where each battery cell is at nominal voltage of 3.2V and capacity of 40Ah. A Battery Management System (BMS) is deployed for monitoring the cells status in the battery pack, including voltage, current, temperature and SOC. The charging process is handled by a three-phase charger with voltage range 60−450V and current range 0−12A. There is a communication channel between the charger and the BMS based on CAN protocol. The BMS transmits the alarm signals to the charger in the case of battery over-voltage, undervoltage, over-heating, etc. The charger will then automatically reduce the charging current or voltage and eventually turn off the process.

The discharge process of the battery is handled by an electronic load with voltage range of 0−60V, current 0−120A and rated power at 2400W, with manually/remotely programmable capability. The electronic load is used under constant current mode. In this mode the current is only adjusted at the beginning and then remains constant until the end of testing. A minimum voltage condition can be also applied to protect the battery lifetime once the battery is completely discharged. The whole test setup is shown in Fig. 9.

In addition, a temperature probe and several thermistors are available to monitor the temperature at different cells for the testing of the battery pack. A PC software is used to log realtime data of battery status, with minute resolution. Preliminary tests have been carried out to verify the battery charging and discharging characteristics with temperature measurement.

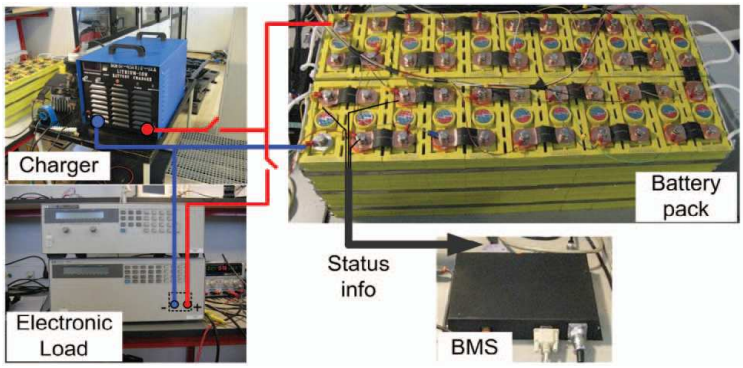

Figure 12. Laboratory configurations for battery characterization

4.3.1 INITIAL TESTING RESULTS

Initial testing results are listed here. It has to be mentioned that although for the sake of brevity not all the results are shown in this report, all of them have been used for parameterization of the battery.

4.3.1.1 TEMPERATURE MEASUREMENT FOR 1C-DISCHARGING:

In this test, the temperature behavior of an LFP cell is measured and recorded with a constant current (CC) discharging cycle using the electronic load of Fig. 9, with current fixed to 40A. The LFP cell is discharged from SOC of 80% down to 2.5V , which is the minimum recommended discharge voltage claimed by the manufacturer. The test was conducted at the ambient temperature of 22°C. From graph of Fig. 10 it is observed that the temperature increases linearly through the whole discharging period, which is about 52 minutes, and the final battery temperature is about 37°C. This test is to verify the cell temperature variation during the discharging period.

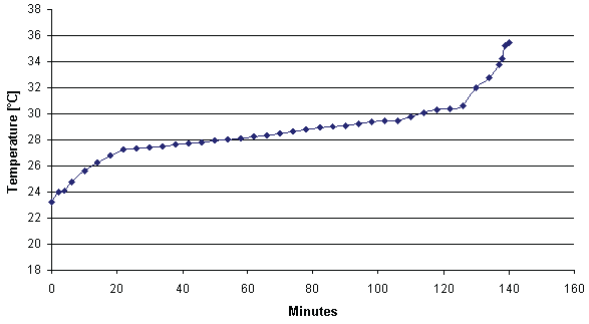

Figure 13. Temperature trend of LFP cell, discharging at 1C rate, ambient temperature of 22°C.

4.3.1.2 TEMPERATURE MEASUREMENT DURING 0.5C-CHARGING:

Another test performed is charging test on the same LFP battery. The cell is charged using a power supply set at CC mode, with charging current at 0.5C 20A. The battery is charged from 20% SOC, where battery is at the minimum discharge voltage, up to 4.25V , which is the maximum battery charge voltage. The test is conducted under ambient temperature at 23°C. The result is shown in Fig. 11.

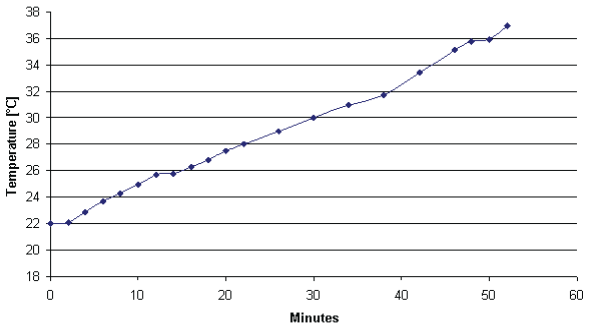

Figure 14. Temperature trend of LFP cell, charging at 0.5C rate, ambient temperature of 23°C.

From the graph of Fig. 11, it is seen that during the charging cycle the temperature show similar characteristics as discharging cycle, while entailed a final temperature about 36°C and a charging time about 140 minutes.

Further test done includes the battery open circuit voltage test. The result is shown in Fig. 12. From the figure, it can be seen that the ampere hour values are different during the charging and discharging process. This discrepancy can be used to describe the battery charging efficiency,

$$\eta = \int i_{\text{discharging}} dt \Big/ \int i_{\text{charging}} dt \times 100\%$$

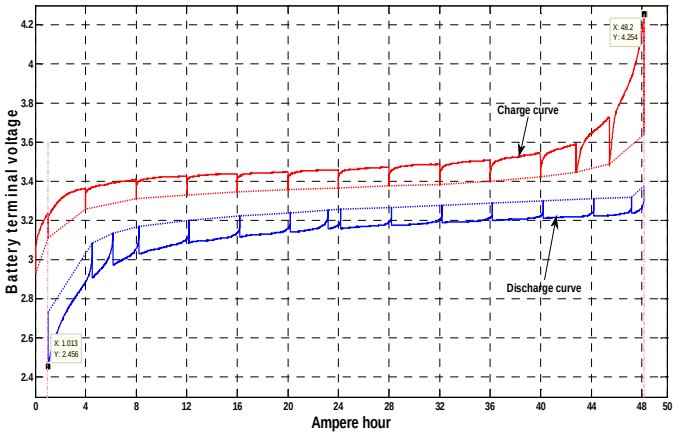

Figure 15. Voltage measurements based on Ampere hour

The data obtained in this section was used in Section 5.1 and 5.2 to form the experimental input to construct the battery models.

5 BATTERY MODELING

The Battery Modeling work is divided in two main parts: The first part describes the battery degradation and SOH model and the second part describes the dynamic behavior model.

5.1 BATTERY DEGRADATION AND SOH MODEL

This section describes the model which can be used to predict thermal effects and degradation in electric vehicle (EV) batteries

5.1.1 ABSTRACT

The work presented here is based on a model-study aimed at obtaining a better understanding of electric vehicle (EV) battery performance and degradation effects, amongst which thermal effects are central. The model is intended to serve as a simulation tool, as well as a data collection on degradation effects.

It has been the aim of this model, to include degradation effects which may be quantified by the use of degradation measurements and to enable a study, of the influence that vehicle-to-grid (V2G) operation will have on lifetime and performance of EV batteries. An initial analysis of such operation has also been made.

5.1.2 INTRODUCTION

The prospects of using EV batteries as buffer or storage units in the electric power system have been described and investigated [1]. It raises the question of how this will affect battery life, and for that purpose a simulation model can be very useful in order to evaluate the effects that use-pattern has on EV battery degradation, lifetime and performance.

From a user perspective, the important parameters relating to an EV battery are e.g. remaining energy capacity, remaining lifetime and efficiency. These parameters are strongly dependent on a number of variables, such as temperature, depth-of-discharge (DOD), charge and discharge rates and cycle number. All of these effects, as well as several others, add up in a complex manner to result in the observed performance of the battery.

This means that battery use affects battery performance and vice versa. The work presented here is aimed at creating a model that will enable a closer study of degradation effects, amongst which the thermal effects are central. The model incorporates a user interface and is intended to serve as a simulation tool, as well as a data collection on degradation effects.

5.1.3 THEORETICAL BACKGROUND

It has been established [2, 3] that the energy capacity fade and increase in internal resistance of the individual battery cells - which are indicators of the use of battery life - are dependent on factors such as charge/discharge rate (C-rate), depth-of-discharge (DOD), temperature and number of charge/discharge cycles.

The physical processes resulting in degradation are to a large extent related to the cell electrodes. The charging and discharging processes lead to phase changes within the electrodes, which in turn result in inhomogeneous volume changes. These volume changes cause microscopic voids and cracks which reduce the overall electrode contact area and lead to capacity fade and increase in internal resistance of the cells. Temperature variations will tend to have similar effects due to differences in thermal expansion coefficient. The following aging effects have so far been taken into consideration in the model presented here:

- Depth of discharge (DOD)
- Number of cycles
- State of charge (SOC)
- C-rate
- Temperature & temperature cycling
- Time as such

The cycle number and depth of discharge of the individual cycles are interconnected as a battery degradation mechanism. In order to model this, a so-called rain-flow-counting algorithm [4] has been implemented in the model. This algorithm counts and sorts charge cycles according to DOD, after which a lifetime consumption weight factor is attributed to each cycle.

The rain-flow-counting approach to estimating degradation is normally used when calculating mechanical degradation. In the case of battery cells, the degradation mechanisms are similar [5] and this method is therefore expected to provide a realistic picture of the degradation process.

5.1.4 THERMAL CHARACTERISTICS

A thermal model of an EV battery requires thermal properties of the individual cells to be determined. A Li-ion battery cell was tested in order to determine its thermal properties. This was done by placing a resistive heat source on one side of the cell and measuring the transient temperature response on the other side of the cell. A

calculation model was then calibrated against the measurement results to obtain the relevant values. A fairly accurate description of the thermal characteristics of a collection of battery cells is given by equation 1:

$$\frac{dT}{dt} + \alpha \cdot T = \beta \qquad \text{eq.1}$$

With α and β being constants determined by thermal capacity (C), thermal conductivity (λ), mass density (ρ), ambient temperature (T_a) , density of dissipated power (P_v) as well as the geometry of the cell collection. A change in ambient temperature or dissipated power of the battery will result in a transient response with a temperature distribution that exponentially approaches a steady state value:

$$T(t) = exp\left(\frac{-t}{\tau}\right) \cdot (T_0 - T_\infty) + T_\infty \qquad \text{eq.2}$$

With T_0 being the initial temperature and T_∞ the steady-state temperature. The parameter (τ) is a thermal time-constant determined by thermal capacity, mass density, thermal conductivity and cell geometry. The tested cells were found to have a thermal conductivity of app. λ ≈ 0.4 W/(m·K) and a thermal capacity of app. C ≈ 1400 J/(kg·K). For a single cell of the type tested here this leads to a time constant (τ) in the range of:

$$\tau = \frac{\rho \cdot C \cdot d^2}{\lambda} \sim 1h \qquad \text{eq.3}$$

With *d* being a characteristic dimension of the cell. For a large collection of battery cells the time constant becomes even longer and this means that thermal equilibrium will usually not be obtained. Transient modeling is therefore essential when describing the battery thermally. Figure 1 shows how a thermal model has been adjusted to fit the results of a test and thereby determine the thermal properties of a battery cell.

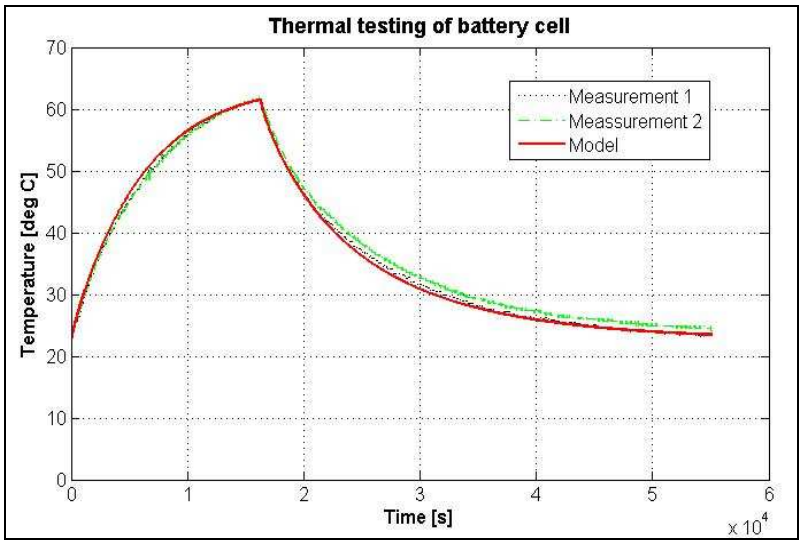

Figure 1: Comparison of test- and calculation of the thermal response of a Li-ion battery cell.

The thermal part of the model is based on the finite-difference method, with the battery cells being placed in a 2D-array. Each battery cell constitutes a thermal element as illustrated in figure 2. This means that possible hot-spots within the individual cells are not included in the analysis.

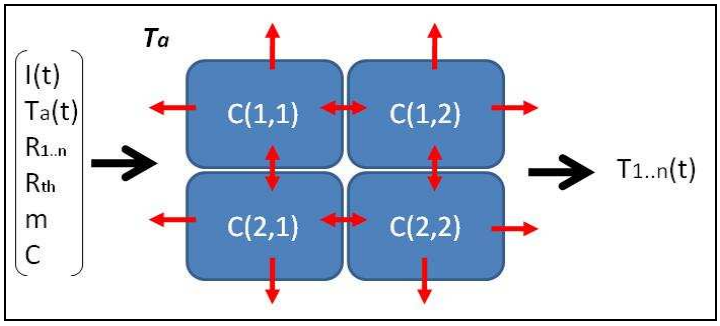

Figure 2: Heat exchange between cells in a 2D-array.

Each cell is seen as a homogeneous medium with a certain thermal capacity and thermal conductivity. Each cell is also assumed to contain a heat source dissipating a power of:

$$P_{cell} = I^2 \cdot R_i \qquad \text{eq.4}$$

With I being the cell current and R_i the internal cell resistance, which is typically in the range of a few mΩ. In addition to joule heating resulting from the internal resistance, a reversible heat effect may also be taken into account [6]. The reversible heat pr. mass unit is given as:

$$q_{rev} = T \cdot \Delta S = n \cdot F \cdot T \cdot \frac{dV_{oc}}{dT} \quad \text{eq.5}$$

With n being number of electrons pr. molecule of reactant, F [C/kg] is the Faraday constant, T is temperature and V_{oc} is the open-circuit-voltage. Depending on the type of battery dV_{oc}/dT may be either positive or negative, if $dV_{oc}/dT > 0$ the effect will heat when charging and cool when discharging. The size of the reversible heating effect may be found experimentally by measuring dV_{oc}/dT but it is usually negligible compared to the irreversible (joule) heating.

The cell voltage has been modeled by subtracting the voltage drop across the temperature dependent internal resistance from the open-circuit-voltage (V_{oc}), while V_{oc} may be calculated using the Nernst equation (eq.7) [6]:

$$V_{cell} = V_{oc} - I \cdot R_i(T) \quad \text{eq.6}$$

$$V_{oc} = E_0 + \frac{R \cdot T}{n \cdot F} \cdot ln\left(\frac{A_p}{A_r}\right) \quad \text{eq.7}$$

Were E_0 is a cell-specific constant and R is the gas constant. The variables A_p and A_r are the reactivity products of products and reactants respectively. If a linear relation between reactivity product and state-of-charge (SOC) is assumed this leads to a relation between SOC and open-circuit-voltage which is show in figure 3.

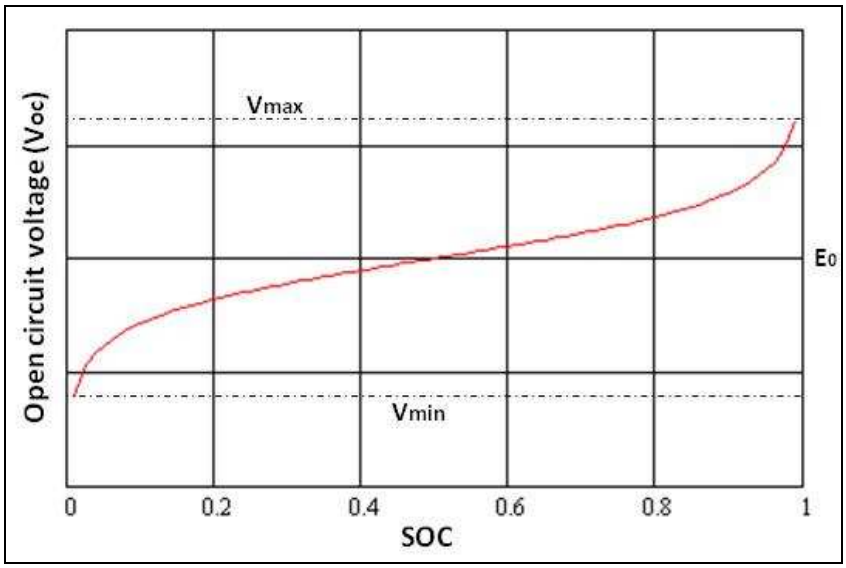

Figure 3: Open-circuit-voltage variations with SOC level.

5.1.5 DEGRADATION EFFECTS

The thermal part of the model has been integrated in the main program that consists of a time-loop in which electrical properties, degradation effects and thermal properties are calculated in each time step. Figure 4 shows a graphical representation of the model. Besides the thermal and electrical parameters, main inputs are the charge/discharge current profile as well as the ambient temperature profile.

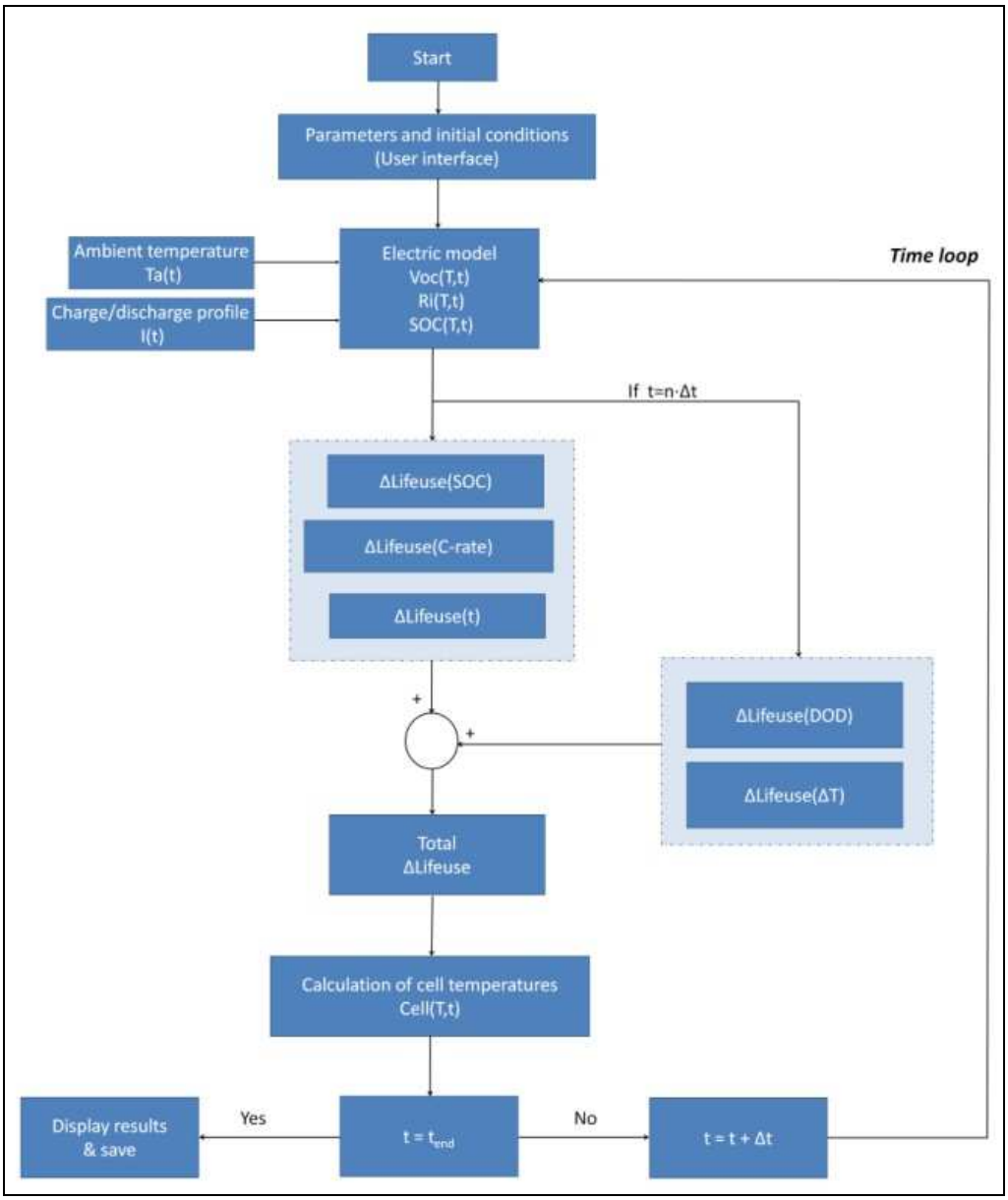

Figure 4: Sketch of the battery model.

Since thermal effects, and in particular degradation effects, have rather long timescales, a relatively large time-step, of e.g. 5 minutes, will provide sufficient time-resolution to accurately capture the dynamic effects. The time-loop contains an equation based description of the degradation effects with the formerly mentioned rain-flow counting algorithm as a central part. The rain-flow counting calculation is rather time-consuming and it is therefore

only activated at certain time intervals. Degradation is assumed to result in reduced battery capacity and increased internal resistance.

Besides the degrading effects resulting from SOC cycling and thermal cycling, the C-rate in itself is thought to have a degrading effect. This might in part be attributed to local heating effects in the electrodes leading the mechanical degradation caused by uneven thermal expansion.

The assumption that time, as such, has a degrading effect, should probably be seen more as a recognition, of the fact that all the degrading effects, which are acting together in a complex manner, to some extend are taking place even when the battery is in an idle state.

Typically, end-of-life is associated with a decrease in capacity to 80% of the original value. Simulating a typical use-pattern for a representative amount of time, e.g. a few months, and observing the corresponding reduction in battery capacity, will make it possible to extrapolate to end-of-life and thereby establish a link between use-pattern and battery lifetime. A thorough investigation of issues related to battery modelling may be found in [7].

5.1.6 MODEL DESCRIPTION AND USE

The battery model has been implemented in MATLAB and includes a graphical user interface. The main user interface is shown in figure 5.

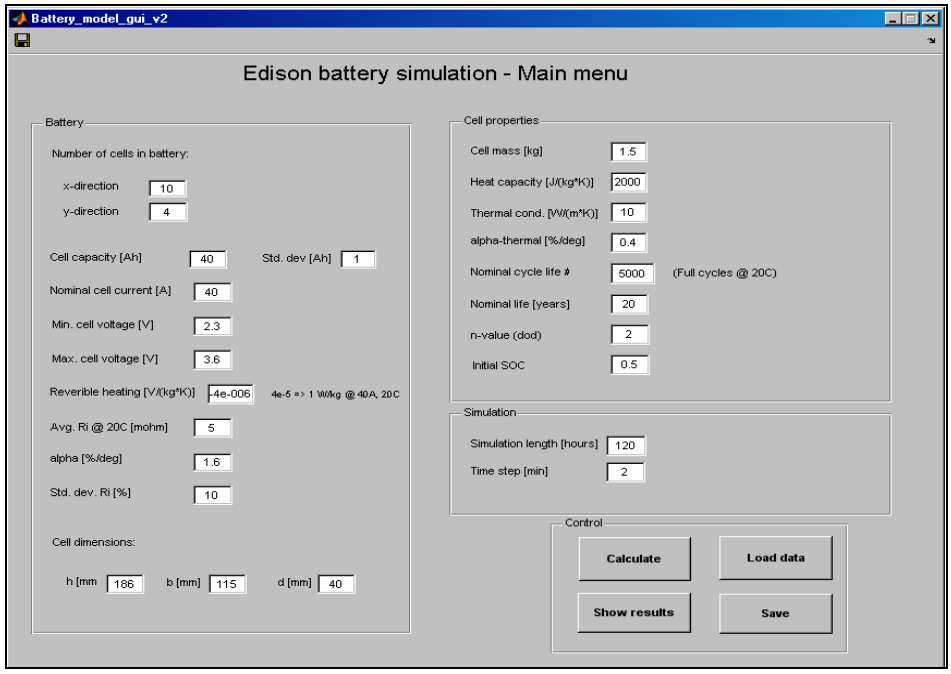

Figure 5: Main user interface of simulation model.

The main menu allows for change of various parameters and simulation settings. This includes statistical variations of initial cell properties, such as, internal resistance and charge capacity.

The program allows the user to load pre-defined charge/discharge profiles. The user also sets a simulation length in the main menu. If the simulation length is longer than the charge/discharge profile, the program will repeat the profile until the end of the simulation time. With a 2-minute simulation time step it takes a few minutes to calculate a simulation sequence of 120 hours on a laptop computer. An output window allows for presentation of the simulation results, as shown in figure 6.

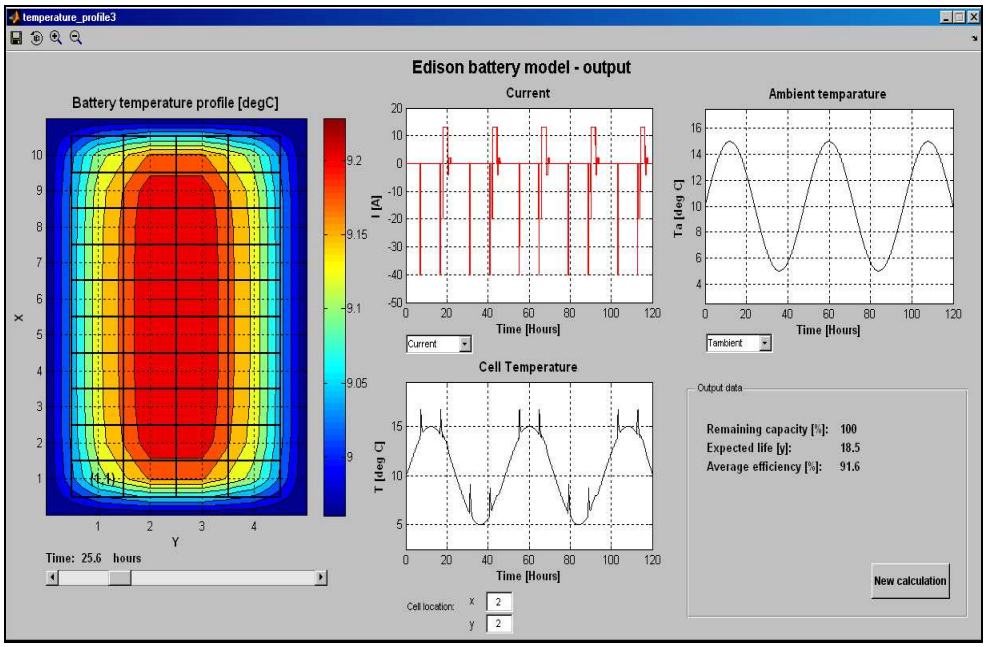

Figure 6: Model output interface.

The output interface allows the user to view different outputs in the form of graphs. The temperature profile of the battery at different times during the simulation can be viewed by shifting the bar in the lower left side of the window. The contents of the two graphs in the top of the window can be changed by using the corresponding drop-menus and the bottom graph in the middle shows the temporal temperature development of individual selected cells.

5.1.7 SIMULATION RESULTS

Various test-runs have been performed in order to verify that the model results are in accordance with logic and commonsense reasoning. Figure 7 shows a contour plot of temperature distribution during operation, inside an array of 4x10 cells. The long time-constant and variations in ambient temperature and current, results in a continuously changing internal temperature profile. Differences in internal resistance and capacity amongst the cells result in a non-symmetrical temperature distribution across the array.

When the battery is exposed to "normal" operation, in which discharging is only related to driving, the internal temperatures do not diverge much from ambient temperature. This is due to the combination of relatively low losses (in the range of ~10%) and high thermal capacity of the cells.

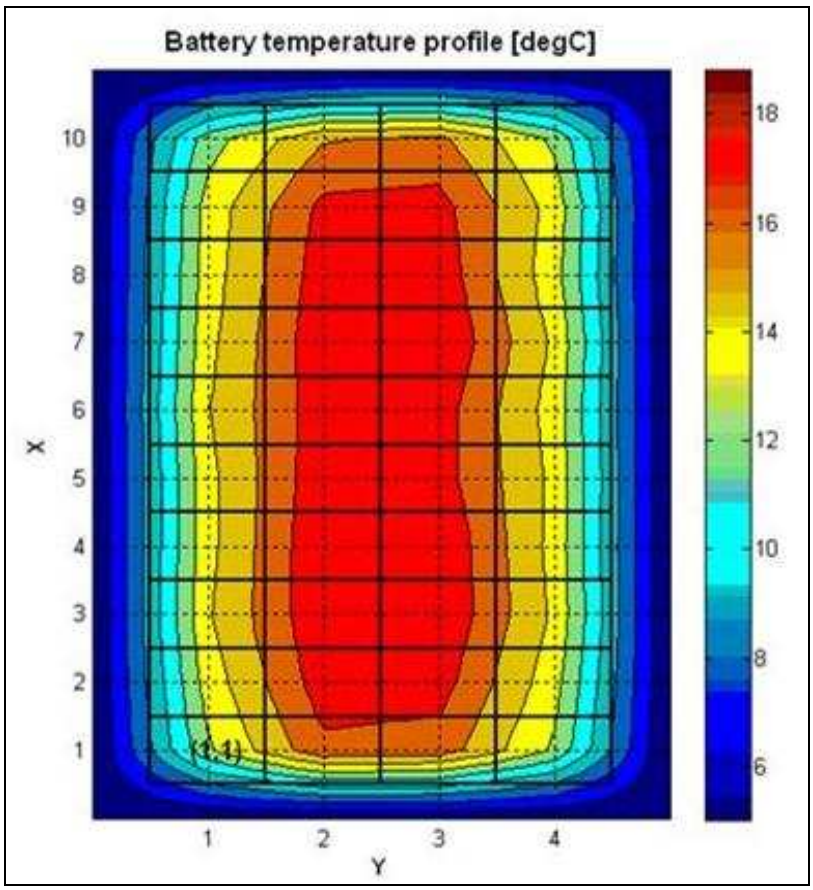

Figure 7: Contour plot of temperature distribution within a battery cell array.

If the battery is exposed to a more continuous sequence of charge and discharge, as expected when performing V2G operation, the battery core temperature tends to stay a few degrees above ambient. This is indicated in figure

8 where the result of a 120-hour test-run is shown. The simulated charge/discharge pattern is the result of combined driving and V2G operation.

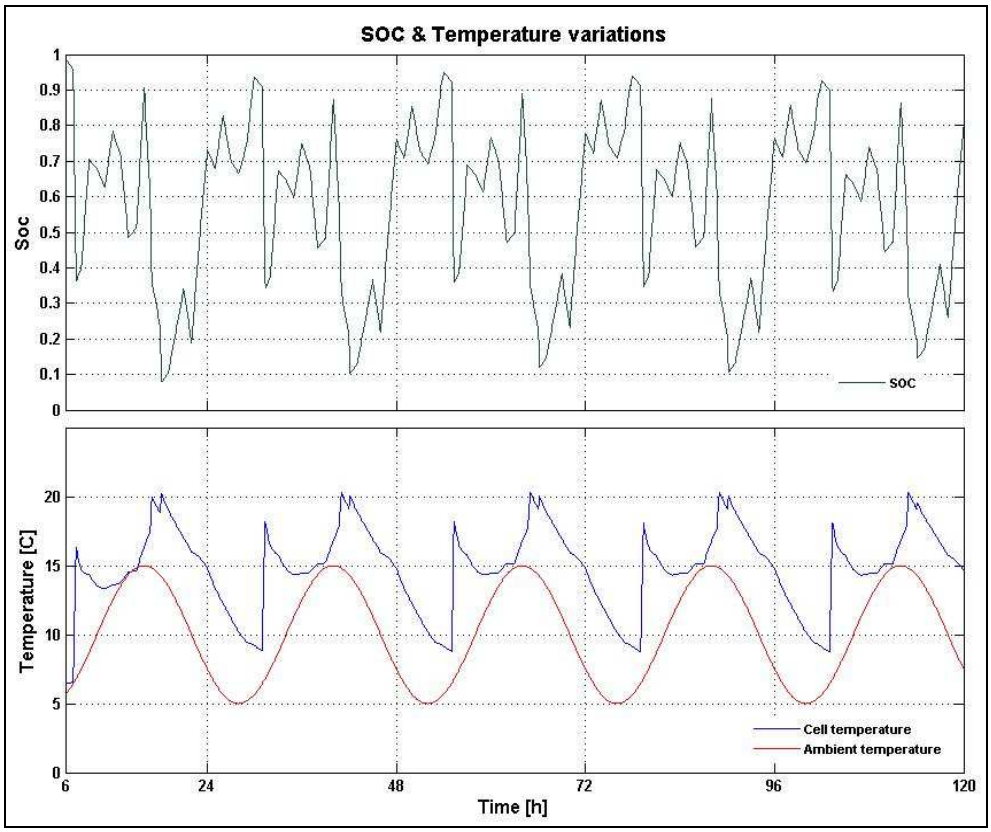

Figure 8: Simulated state-of-charge (SOC) and core temperature of an EV battery with combined driving and V2G operation.

The simulations show, that such semi-continuous operation leads to an over-all increase in efficiency because of a temperature increase which leads to reduced internal resistance. The cost and user experience with regard to driving are related to a number of important parameters which are closely interrelated in a complex manner:

- Energy content
- Maximum power
- Efficiency
- Battery degradation (lifetime)

The simulation model presented here enables a closer study of these relations but this has yet to be done.

In order to obtain an indicative result with regard to the effect of use pattern, 5 different charge/discharge profiles has been simulated. Each profile had a length 24 hours but they were repeated 7 times to reach a total simulation length of 168 hours, The 5 profiles, which were artificially made to indicate the effect of different use-patterns, are listed in table 1.

Profile	*Description*
1	**Work-home driving profile with relatively fast charging in the evening.**
2	**Work-home driving profile with slow charging during both day and night.**
V_2G1	**The same as 2 but with vehicle-to-grid operation resulting in random inter-hour SOC variations of ±0.15.**
V_2G2	**The same as V_2G1 but with SOC variations of ±0.2.**
V_2G3	**The same as V_2G1 but with SOC variations of ±0.25.**

Table 1: Overview of test simulation profiles.

The SOC profile simulations should only be regarded as rough indicators of how such operation might affect battery life, as well as an indication of how a through simulation based analysis can contribute further. Figure 9 shows profiles 2 and V_2G1.

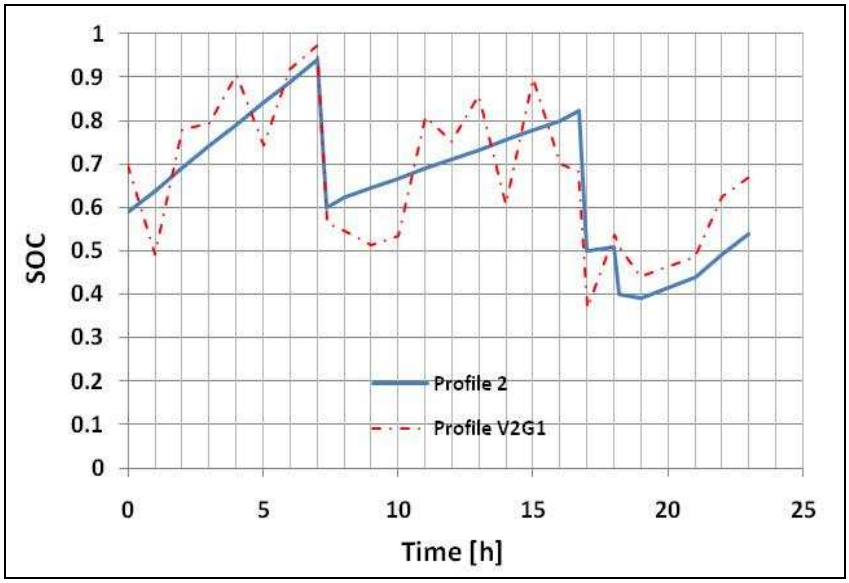

Figure 9: Two of the simulated SOC profiles.

The simulated battery contained 40 cells, each with a capacity of 40Ah. The cycle-life at 100% DOD was set to 5000 cycles. Results from the 5 test simulations are listed in table 2. It shows a significant reduction in battery life as a result of V2G operation, which is not surprising since it leads to an increased number of partial cycles. The effect of day-charging and slow night charging, on the other hand, is to increase the expected lifetime. This is because it lowers the over-all C-rate and reduces the depth of discharge level.

Profile #	**1**	**2**	**V_2G1**	**V_2G2**	**V_2G3**
Expected life [y]	**19.8**	**27**	**14**	**10.7**	**9.7**
ε_{ff} [%]	**90.8**	**94.1**	**91.4**	**94.8**	**95.5**

Table 2: Results from test simulations.

The life-time reducing effect of increased depth of discharge level can be also seen from the fact that increased size of the V2G SOC variations result in significantly shorter lifetime.

The over-all efficiency of the battery is higher for profile 2 than for profile 1. This is not surprising since both DOD and C-rate during charging is lower for profile 2. But surprisingly, there is the opposite tendency for the three V2G profiles. Beyond a certain point, larger SOC cycles seem to result in higher efficiency. This behavior is explained by the fact that more-or-less continuous operation results in higher cell temperature and thereby lower internal resistance. These examples illustrate the complexity of this system of interrelated and sometimes counteracting mechanisms and the usefulness of a simulation model.

5.1.8 CONCLUSIONS

The simulation model presented here has so far not been subjected to a representative selection of test cases. In addition to that, the implemented equations describing cell degradation mechanisms are so far based entirely on data obtained from publications and not on empirical data from a specific cell type. It is thus too early to draw any exact conclusions with regard to the influence that use pattern has on lifetime.

The main purpose of this work has been to make and test a simulation model which will enable a closer study that can lead to exact conclusions with regard to the effect that use pattern has on battery lifetime and performance. In that sense this work has been successful. The model will clearly be able to assist in at least two important areas;

one is to complement experimental results to obtain a clearer picture of how the different mechanisms influence battery aging and the second is to determine how battery use-pattern affects aging.

The initial model studies indicate a 50% reduction in battery life as a result of V2G operation. A more detailed study might show how to prolong battery life and improve efficiency. Changing the model equations to include measurement based inputs is a manageable task which can be done gradually as more knowledge is gained.

5.1.9 REFERENCES

[1] W. Kempton, J. Tomic, S. Letendre, A. Brooks & T. Lipman: "Vehicle-to-Grid Power: Battery, Hybrid, and Fuel Cell Vehicles as Resources for Distributed Electric Power in California", Online Report, 2001.

[2] F. Marra, C. Træholt, E. Larsen & Q. Wu: "Average Behaviour of Battery-Electric Vehicles for Distributed Energy Studies". Innovative Smart Grid Technologies Conference Europe (ISGT Europe), IEEE PES. Gothenburg, Sweden. 2010.

[3] D. U. Sauer & H. W. Wenzl: "Comparison of different approaches for lifetime prediction of electrochemical systems - Using lead-acid batteries as example". Journal of Power Sources, 2007.

[4] S. D. Downing & D. F. Socie: "Simple rain-flow counting algorithms". International Journal of Fatigue, Volume 4, Issue 1, January 1982.

[5] M. Safari, M. Morcrette, A. Teyssot & C. Delacourta: "Life Prediction Methods for Lithium-Ion Batteries Derived from a Fatigue Approach". Journal of the Electrochemical Society, 2010.

[6] M. Winter & R.J. Brodd: "What Are Batteries, Fuel Cells, and Super Capacitors?" Chemical Reviews, 2004, Vol. 104, No. 10.

[7] N. A. Chaturvedi, R. Klein, J. Christensen, J. Ahmed & A. Kojic: "Algorithms for advanced battery-management systems – Modeling, estimation and control challenges for Lithium-ion batteries". IEEE Control systems magazine, June 2010.

5.2 BATTERY MODELLING – DYNAMIC PERFORMANCE

Previous section details the battery characteristics in terms of thermal and driving pattern. In this section, the SOC modeling of the battery is detailed and parameterization procedure is described. The battery model(s) will be implemented in Matlab/Simulink and represent the different chemistry of batteries used in the Edison project under the circumstances described below as well as mentioned in the purpose description above.

In the following the model of dynamic performance of battery modeling will be described including different battery models suggested in literature, construction of a complete battery model and parameterization of the battery model(s).

5.2.1 DEMANDS FOR THE BATTERY MODEL

The battery electric characteristics, longevity, and runtime are affected by different chemistries, ambient conditions, as well as driving and charging patterns. The modeling work basically includes two elements as indicators of battery status, state of charge (SOC) and state of health (SOH). The SOC identifies the available capacity of battery while SOH indicates the battery performance status including actual usable capacity and runtime.

5.2.1.1 BATTERY CHEMISTRIES

Several different chemistries are used for battery applications. A great part of these are described in “WP 1.1 Electric Vehicle Technology”. How many of the battery chemistries that should be represented in the Edison project must thus be considered.

For the work of WP 6a Lithium-ion batteries have been purchased. These are of the types “Lithium Iron Phosphate” (LFP) and “Lithium Cobalt Manganese Nickel Oxide” (NMC) and should be the main focus of the battery modeling in WP 1.5.

Note: The expectation is that lithium-ion chemistries will in the future represent the primary use of battery technology for electrical vehicles as this type of battery offers the highest energy density for electrical vehicle use [17].

5.2.1.2 VI-CURVE

The volt-current charge and discharge curve describes the electrical behavior of the battery and are affected by temperature, charge/discharge rate, charge/discharge cycle number, storage time and SOC (state of charge). All these factors should be considered in the battery model.

Note: Charge and discharge cannot necessarily be modeled by the same model. This is dependent on the type of battery and the hysteresis of the battery.

5.2.1.3 BATTERY IMPEDANCE

It has been requested by the Edison project that the battery impedance is also modeled by the battery model. As the V,I characteristic will be modeled as described above, the impedance will also be known.

5.2.1.4 *AGING* - AVAILABLE BATTERY CAPACITY - CYCLE AGING

Aging must be represented in the battery model, through thermal, cyclic and storage aging. These aspects are all covered by the battery model presented later in this paper.

Note: A common limit for determining the number of cycles a battery can operate for is a reduction in the batteries maximum capacitance to 80 % of the batteries original (or data sheet specified) capacity [7].

5.2.1.5 POWER LOSSES (SELF-DISCHARGE)

Power losses and self-discharge are also of interest to the Edison project. The self-discharge is not represented in the battery model presented later in this document but could however be implemented. The power losses can be estimated by the battery current and impedances.

Note: According to [16] commercially available Li-ion battery cells showed a self-discharge resulting in a reduction of 3 % of the initial capacity over 30 days. It was therefore concluded that self-discharge effects are insignificant for applications where the battery is used often. A example self-discharging curve is shown in Fig. 11.

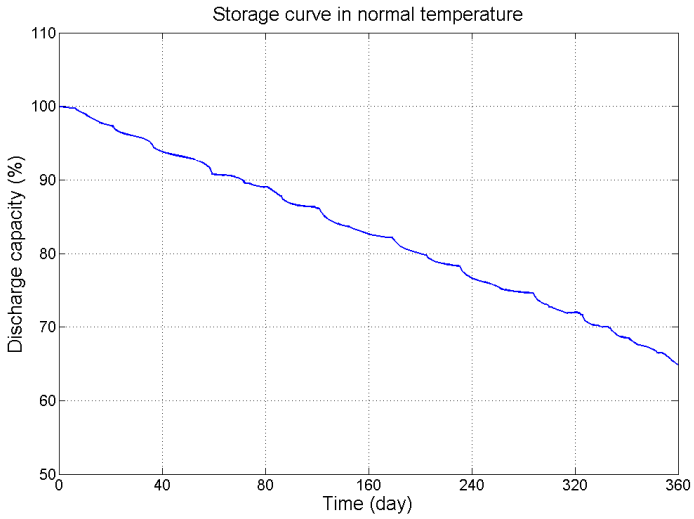

Figure 16. Battery discharge capacity versus the stored date.

5.2.2 BATTERY CELL MODELS DESCRIBED IN LITERATURE

The most promising battery systems for EVs and plug-in hybrid electric vehicles (PHEVs) are based on lithium-ion or lithium-polymer battery, which models are focused in this paper. A variety of battery models are proposed in literature to capture the battery characteristics from different perspectives. This model classification is inspired by [6] and different classification is used in [Ravishankar2003] which gives a good overview of different battery models. Roughly, these models can be classified into electrochemical [1], [2], [3], mathematical [4], and equivalent electric circuit models [5], [6], [7] to serve different study purposes.

For grid impact studies, the battery model shall be kept as simple as possible in order to facilitate the simulation of large amount of EVs into the grid; while from the owners, it is much desirable to know the current battery SOC and SOH, as well as the battery runtime prediction [8]. Electric circuit models are seen as an intermediate approach [5] between electrochemical and mathematical models where the model accuracy, in the range of 1-5% [6], and computational efficiency are balanced. In [5], electrical and thermal properties are considered in the model formulation, where the equivalent circuit consists of a RC circuit with a series resistance. The work in [6] extended the work in [5] with two RC circuits representing the short and long term transients, and the battery runtime is also addressed in the model, however without considering the temperature and cycle number dependency of the model. In [7], the authors include an additional resistance to represent the internal resistance variation with

respect to the increase of cycle number, in consideration of capacity fading due to the time, temperature and cycle number.

It is not the intent to describe the many different models here. Only a short description of the different classes will be given.

5.2.2.1 PHYSICAL/ELECTRO-CHEMICAL

Electro-chemical models include the internal workings of the battery. Thus the physics of the battery is included in electro-chemical models making them very demanding calculations with regard to time and computation power. Electro-chemical models are typically used to optimize the battery composition as the physical design aspects are represented in the model.

These types of models are therefore not seen as a viable option for the Edison project, as the focus of the models are the battery physical design. Furthermore these models are reported as being very time consuming with respect to computation [6], [18].

5.2.2.2 MATHEMATICAL/EMPIRICAL

According to [6] mathematical models are generally very abstract with very little practical meaning. They can be used for predicting battery runtime, efficiency and/or capacity. Often mathematical models are developed and only works for specific applications.

Mathematical battery models are therefore not, it would seem, an option for the battery model to be used in Edison WP1.

5.2.2.3 ELECTRICAL-CIRCUIT

Electrical-circuit models are based on representation of the battery by and electrical circuit. This often takes form in a controlled voltage source that varies the voltage with the SOC of the battery. The voltage source is connected in series with resistances and RC circuits modeling the voltage response of the battery.

Dependent on the layout of the electrical circuit they can further be classified as; Thevenin-based, Impedance-based, runtime-based or as a mixed model. For more information [6] and [18] should be consulted.

5.2.3 EXISTING BATTERY MODEL INCLUDED IN MATLAB

A battery cell model is included in the Matlab simulink SimPowerSystem package. This model is based on [14] and consists of a simple electrical circuit (Thevenin-based). The circuit is based on an internal resistance in series with a controlled voltage source. The model is depicted in Figure 17.

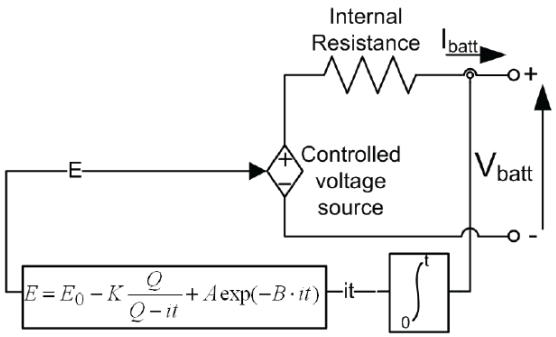

Figure 17 Non-linear battery model from [14]

The internal resistance is a constant either supplied directly from the manufacturer or it can be evaluated from the battery efficiency, nominal voltage and nominal capacity with a reasonable precision according to [14].

The controlled voltage source represents the SOC dependent no-load voltage of the battery and is based on coulomb counting (integration of the current through the battery). The expression for the no-load voltage, *E*, is given in Figure 17 as well as in the equation below.

$$E = E_0 - K\frac{Q}{Q - \int_0^t i \cdot dt} + Ae^{-B \cdot \int_0^t i \cdot dt}$$

The no-load voltage is dependent on the battery constant voltage, E_0, the polarization voltage, *K*, the battery capacity, *Q* [Ah], the exponential zone amplitude, *A* [V], the exponential zone time constant inverse, *B* [Ah^{-1}], the time, *t*, and the current through the battery, *i*. For further explanation, see [14].

Parameters for several different battery chemistries and different cell sizes as well as explanation of the parameterization are included in [14]. In general the charge and discharge curves for the battery cell and basic information on cell capacity should be sufficient for the parameterization.

The model implemented in Matlab can take into account several different chemistries and sizes of the batteries and thus represent a fast and easy avenue for creating a battery model.

The capabilities of the [14] model are limited to describing the charge and discharge curves of a battery cell at constant temperature and aging. The model can represent the transient state of the battery cell. The level of accuracy is though unknown and will be very dependent on the available operation information from the manufacturer. Furthermore the electrical circuit model seems very simplified compared to other electrical circuit models of battery performance, this is however also the strength of the model with regard to parameterization.

5.2.4 SUGGESTED BATTERY MODEL IMPLEMENTATION IN MATLAB

The most commonly suggested battery models for investigation of the performance of electrical vehicles are based on (mixed) electrical circuit models. These are more advanced than the simple electrical circuit model presented in the previous sections, as the circuit is expanded with one to three resistances in parallel with a capacitance to model the transient response more accurately.

Given the advantages of electric circuit type of model, it is deployed in this work for the simplicity and accuracy. Intuitively, the accuracy of battery model can be enhanced in proportional to the complexity of the configuration of the equivalent circuits, however, the increasing complexity will also reduce the computational efficiency. The work in [9] studies the model accuracy with respect to the number of RC circuits and it is found that 2 circuits can reasonably replicate the battery behavior with less than 10% error while preserving fast computational speed.

The deployed equivalent circuit model is based on the work in [6]. Comparing with the work in [6], an additional series resistance is included in the model to represent the variation of the internal resistance resulting from cycle number and temperature [7], [10]. Fig. 12 illustrates the proposed equivalent circuit.

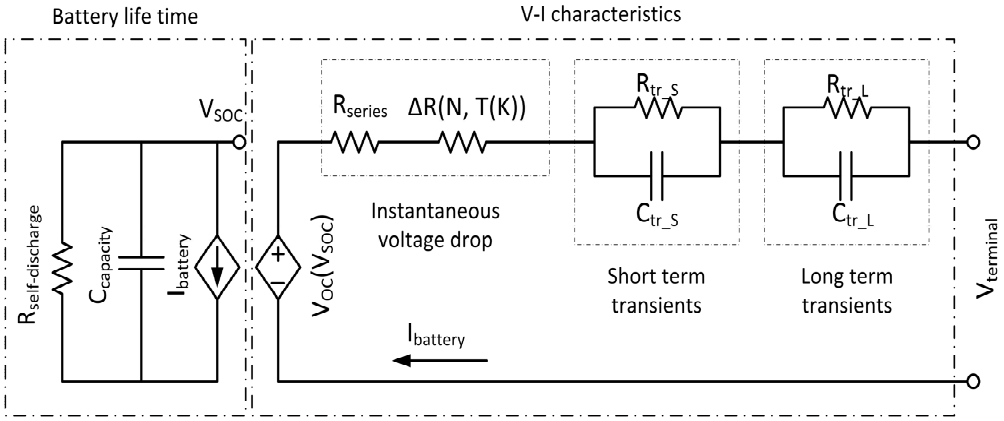

Figure 18. The equivalent circuit model proposed in this project

The left side of the model represents the battery current SOC level, while the right side describes the battery V-I characteristics during charging/discharging. $C_{capacity}$ represents the current capacity of the battery, where the inputs for this shall be coming from the battery SOH model.

5.2.4.1 BATTERY V-I CHARACTERISTICS MODELLING

R_{series} → *Describe the instantaneous terminal voltage drop of the step current under normal temperature and low cycle number;*

$\Delta R(N,T(K))$ → *Describe the change of* R_{series} *due to the cycle number N and ambient temperature T(K);*

R_{tr_S}, C_{tr_S} → *Resistors and capacitors of two RC circuits, describe the transient*

R_{tr_L}, C_{tr_L} *behavior of battery subject to step current;*

$V_{OC}(V_{SOC})$ → *Open circuit voltage as a function of state of charge;*

$C_{capacity}$ → *Usable capacity of the battery, mainly dependent on the cycle number and temperature;*

$R_{self\text{-}discharge}$ → *Battery discharging effect with respect to the calender time;*

The terminal voltage from above model can be calcualted by the equation below,

$$V_{\text{terminal}} = V_{OC}(V_{SOC}) - i_{battery} \times Z_{eq}(SOC)$$

where the Z_{eq} describes the equivalent impedance of the battery, which is a function of the state of charge (SOC). SOC can be calculated based on the equation below,

$$SOC = SOC_{init} - \int (i_{battery} / C_{capacity}) dt$$

where the SOC_{init}, $i_{battery}$, $C_{capacity}$ represent the battery initial SOC, battery current, and the available capacity of battery, respectively.

Theoretically, the battery internal impedance is a function of temperature, cycle number, and *SOC*, which will influence both the steady-state and dynamic characteristics of the battery. In this work, it is noted that in the proposed model, the battery dynamic characteristics resulting from temperature and cycle number of the battery are ignored. Formulae used in the mode are detailed in a sequel.

With the SOC, the open circuit voltage. VOC may be described by the following equation [6],

$$V_{OC} = C_1 + C_2 * SOC + C_3 * SOC^2 + \cdots C_n * SOC^{n-1}$$

where C_1, C_2, …, C_n are coefficients which need to be validated by realistic tests. For SOC dependent impedances, the general expression is below,

$$Z = a_1 + a_2 * e^{SOC * a_3}$$

where *Z* is a general expression of resistance and capacitance of R_{series} and two RC circuits. For every *Z*, the coefficients a_1, a_2 and a_3 will be different and validation is required to confirm the parameters. The $\Delta R(N,T(K))$ is the correction to the internal impedance which is identified based on empirical data.

The total impedance of the battery is

$$Z_{eq} = R_{series} + \Delta R(N,T(K)) + R_{tr_S}\left(1 - \exp\left(-\frac{t}{R_{tr_S}C_{tr_S}}\right)\right) + R_{tr_L}\left(1 - \exp\left(-\frac{t}{R_{tr_L}}C_{tr_L}\right)\right)$$

5.2.4.2 BATTERY AVAILABLE CAPACITY

One of the key issues of the battery model is the expression of battery available capacity. The capacity loss is normally considered coming from two parts, calendar life and battery cycle life loss, and it refers to the irreversible degradation of the battery capacity during rest or cycling operations [7]. The calendar life loss is time- and temperature-dependent while the cycle life loss is essentially related to the cycle number and temperature [11]. The reversible self-discharging of battery is not considered here but may also be considered in the model. An example of battery self-discharging is shown in Fig. 2.

The authors in [4] give a mathematical expression of the calender life loss and cycle life loss. The calender life loss can be roughly expressed by the general equation below,

$$Calendarlifeloss = k_1 e^{k_2 \frac{1}{T(K)}} t^{k_3}$$

where k_1, k_2, k_3 are coefficients, and T(k) represents the stored time (in second).

For EV batteries the cycle life loss is considered more important than the calendar life loss. In literature, cycle life loss is normally modeled based on the physical process [4] or empirical data [12]. In this work, empirical method will be employed to model the loss conforming to the experimental results.

$$Cyclelifeloss = f(N, T(K))$$

The available capacity of the battery can be expressed by,

$$C_{available} = C_{init} \cdot (1 - Calendarlifeloss - Cyclelifeloss)$$

where C_{init} represents the initial capacity of the battery. The battery is usually considered at end of life condition when the capacity is equal or below 80% of the initial capacity.

5.2.4.3 MODEL CONSTRUCTION

A simulation battery model of lithium battery is built in Matlab/Simulink based on the analytical model description of the previous section. The simulation model information, seen as an input-outputs block, are described in Tab. I. The model is An example of changing/discharging simulation curves is shown in Fig. 16. The model is created in Simulink and the basic structure is shown in Fig. 17.

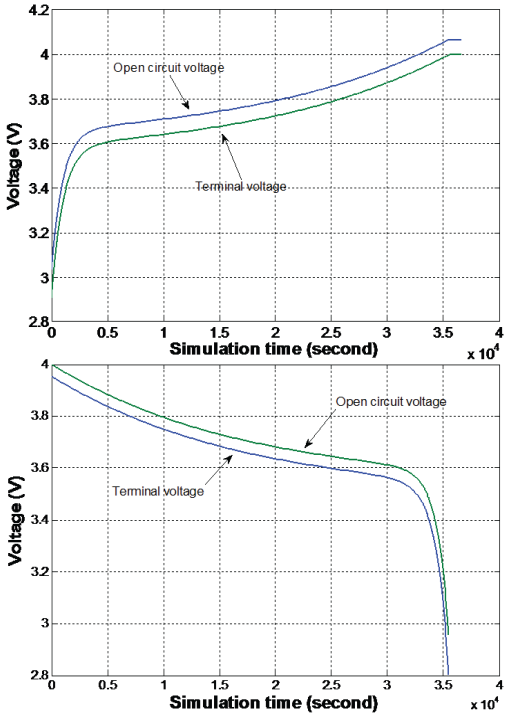

Figure 19. Example charging and discharging curve

TABLE 1. MODEL INPUTS AND OUTPUTS

Inputs	Outputs
• Initial state of charge • Initial battery capacity(Ahr) • Temperature, in Kelvin • Number of used cycles N • Used time (months) • Cut-off voltage(V) • Charging/discharging current(A)	• Battery terminal voltage(V) • State of discharge

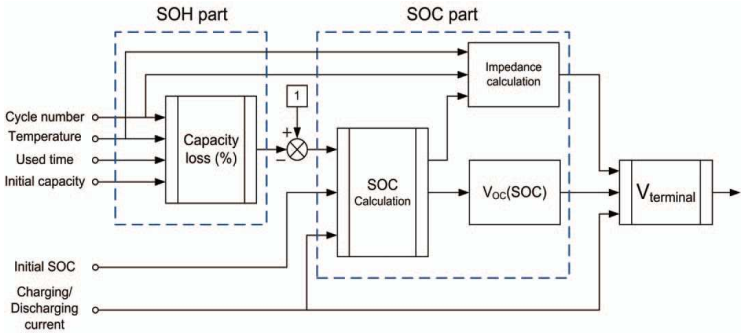

Figure 20. Battery model structure.

5.2.4.4 FROM A BATTERY CELL MODEL TO A BATTERY PACK MODEL

The battery model described in this document is originally intended for modeling a battery cell and not an entire battery pack. The question is then how the full battery pack should be modeled? So far there is limited work on the development of battery pack models. The pack model can either be constructed by combining the appropriate number of cells in series (to increase the voltage across the pack) and parallel (to increase the capacity of the pack). The large amount of the battery parameters will significantly increase the computational burden for the validation work.

Another approach would be to scale the cell model to a pack model. This would include multiplying the voltage of the cell model with the number of cells in series in the actual battery as well as multiplying the capacity by the number of cells in parallel in the actual pack. The second method offers the most flexible with regard to changing the size of the battery pack and will be the method used in the Matlab implementation of the model.

5.2.5 MODEL PARAMETERISATION AND VALIDATION

This section details the parameterisation and validation procedures.

5.2.5.1 MODEL PARAMETERISATION

The parameters presented above are based on a Sony polymer Li-ion battery cell. In the following, how these parameters where obtained will be presented.

5.2.5.2 EXTRACTION OF OPEN CIRCUIT VOLTAGE (V_{OC})

Two methods of extracting the open circuit voltage of the battery are presented in [15], it is however concluded that the following method is sufficient for determining the open circuit voltage. The first method consists of charging or discharging of the battery with built-in pauses for approximately each 10 % SOC of 1 min. During the pauses the voltage will decrease during charging and increase during discharging as can be seen in Figure 21. The voltage should fall/rise to the open circuit voltage if the pause is long enough. In Figure 21 it can be observed that this is not the case, thus the 1 min pause are in reality to short. However by connecting the spikes of the pause by dotted lines and taking the mean value between charging and discharging, it is possible to determine the open circuit voltage with a good accuracy. Further information can be found in [15].

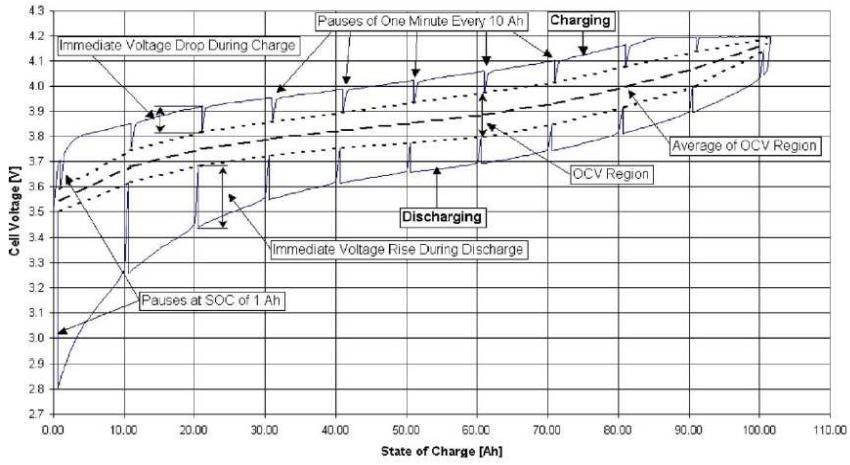

Figure 21 Graphical explanation of determining the open circuit voltage from a discharge curve from [15]

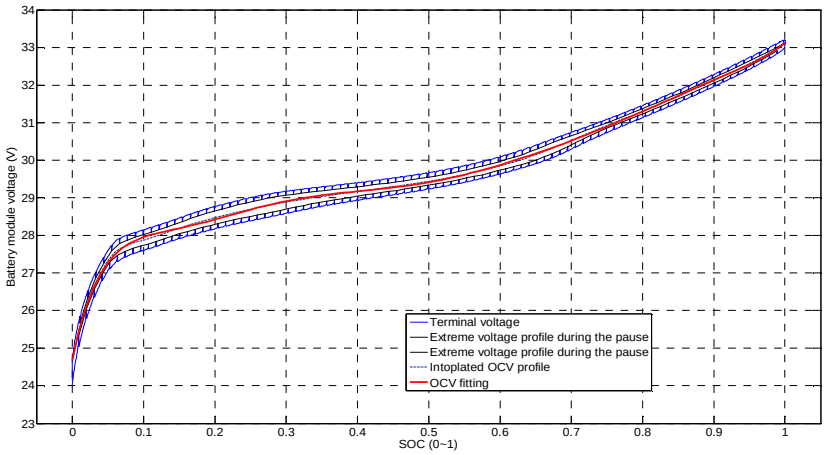

Figure 22. The battery OCV test and fitting result

The fitting result of the open circuit voltage on the NMC module (10 cells in series) is shown in Fig. 19.

5.2.5.3 EXTRACTION OF R_{SERIES} AND RC CIRCUIT PARAMETERS

The extraction of the Rseries and RC circuit parameters (R_{tr_S}, C_{tr_S}, R_{tr_L} and C_{tr_L}) are described in [Schweighofer2003]. The battery is subjected to charging and discharging current pulses of different constant values (0.5-200 A in [Schweighofer2003]) in 5 seconds. As the RC circuit represents the short and long term transient response respectively, the parameters can be found through analyzing the charge/discharge curve. The short term response parameters can be found by looking at the first 0.5 seconds of the response. This also applies for the series resistance which is responsible for the instantaneous voltage rise when the current pulse is applied. The instantaneous voltage rise, U_R, is marked in **Fejl! Henvisningskilde ikke fundet.**. The series resistance can then be found by dividing the voltage with the amplitude of the current pulse. This is under the assumption that the increase in resistance due to cycling has not taken place to a notable degree.

The time constant, τ_D, can be read from the initial slope of the voltage response. Following the voltage amplitude of the short transient response can be evaluated based on the following equation for the voltage response.

$$u(t) = U_R + \hat{U}_D \cdot \left(1 - \exp\left(-\frac{t}{\tau_D}\right)\right)$$

Notice that the long term response can be neglected when looking at the first 0.5 seconds. Following the electrical circuit parameters can be calculated from the equations below.

$$R_{series} = \frac{U_R}{I}$$

$$R_{transient5} = \frac{\hat{U}_D}{I}$$

$$C_{transient5} = \frac{\tau_D}{R_{transient5}}$$

The parameters for the long term transient response can be found in a similar way by analyzing the voltage response in the remaining interval.

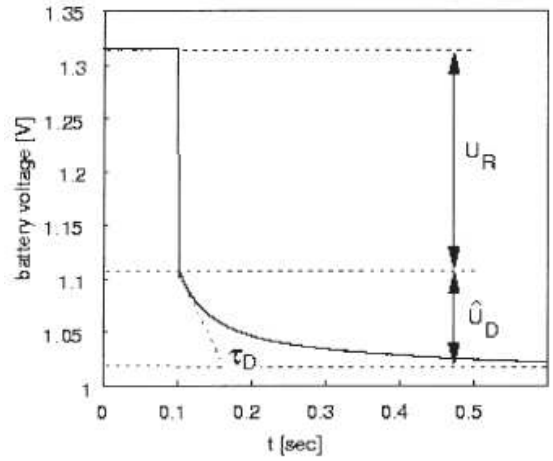

Figure 23 Graphical explanation of determining the electrical circuit parameters from a current pulse response from [Schweighofer2003]

5.2.5.4 EXTRACTION OF CALENDAR LIFE LOSSES

The expression and parameters for the *Calendar life losses* originates from [19] and are based on data from Toshiba on their lithium batteries. It is not clear from [19] how the *Calendar life losses* are parameterized. The expression presented above should be used until information on parameterization is available.

5.2.5.5 VALIDATION PROCEDURE

The developed simulink model needs to be confirmed by the manufacturer data sheet and by the experimental results. The tuning of the parameters is basically a nonlinear curve fitting problem. Due to the large amount of parameters as well as large variation range of parameters involved in the model, it may not be efficient to apply a nonlinear optimisation tool directly for this purpose. For the deployed model, the validation need to be done combining the manufacturer data and experiment such as step current tests to extract the parameters reflects the steady state, dynamic and runtime characteristics of the battery. However, based on the model structure, it is observed that the model can almost be decoupled into SOC part and SOH part, where each of them may be validated separately based on the manufacturer data sheet and test results. In this work, a two-step validation procedure is proposed to validate the whole battery model.

5.2.5.6 VALIDATION OF SOC PART

The validation of the SOC part involves the parameters of V(OC)(V_{SOC}) and impedance parameters R_{series}, R_{tr_S} , R_{tr_L}, C_{tr_S} , and C_{tr_L}. In the first step, the parameters of battery are validated under normal temperature with very low cycle number, and the value of ΔR(N, T(K)) is considered zero. Step current test is required to extract the parameters of the battery, and the discharging curve from the manufacturer data sheet can be used to confirm the steady-state characteristics model. Fig. 21 demonstrates the model for step current test. The final impedance may be confirmed with the electrochemical impedance spectroscopy test.

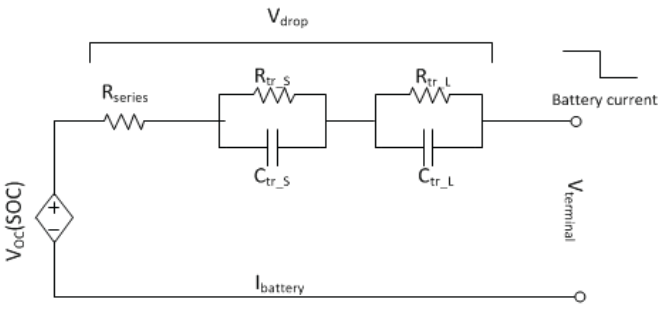

Figure 24. Step current test

5.2.5.7 VALIDATION OF SOH PART

For SOH validation, it is recommended that the validation is done together with the test on ΔR(N, T(K)). The test can also be decoupled into two tests. In the first test, the cycle number is fixed while the battery will be tested under different ambient temperature. While in the second test, the cycle number will be varied under normal temperature. The discharge curve provided by manufacturer under different temperature and cycle number can be used as the reference for the discharging characteristics as well as analyzing the variation of ΔR(N, T(K)) with respect to cycle number and temperature.

5.2.5.8 FUTURE WORK

Generally, the battery steady-state the dynamic characteristics are the function of SOC, cycle number, and temperature [13]. In this work, assumption is made to ignore the difference of dynamic characteristics of the battery at different temperature and cycle number while mainly focuses on the steady state characteristics. In future, this part can be further included in the validation work by performing step current test under different temperature and cycle number to gain the empirical analysis of battery characteristics. Also, for grid integration of EVs, the model of EV shall be at the pack level instead of cell level. However, a solid cell model is the basis to reasonably represent the pack performance. The development of pack model will be mainly based on the real test from both laboratory and real EV charging characteristics. This part of work will be highlighted in the future.

5.2.6 COMMENT AND STATUS ON THEMATLAB MODEL

The battery model is implemented in Matlab as a controlled voltage source in series with a current measurement. The voltage source is controlled by the expression for the open circuit voltage presented above. The reason for this implementation approach is that it is not possible with the SimPowerSystem toolbox to represent variable capacitors and resistors directly (these are included in other toolboxes). Thus all elements of the electrical circuit are represented by their appropriate equations.

Currently all the parameters regarding the V-I characteristics of the model have been parameterised and validated. The temperature effect has not been included in the model as lacking of sufficient experimental data. The next step, the result will be further validated with the result from spectroscopy test result.

5.2.7 REFERENCES

[1] A. P. Schmidt, M. Bitzer, R. W. Imre, and L. Guzzella, "Experimentdriven electrochemical modeling and systematic parameterization for a lithium-ion battery cell," *Journal of Power Sources*, vol. 195, no. 15, pp. 5071–5080, 2010.

[2] S. Bashash, S. J. Moura, J. C. Forman, and H. K. Fathy, "Plug-in hybrid electric vehicle charge pattern optimization for energy cost and battery longevity," *Journal of Power Sources*, vol. 196, no. 1, pp. 541–549, 2011.

[3] M. Urbain, M. Hinaje, S. Rael, B. Davat, and P. Desprez, "Energetical modeling of lithium-ion batteries including electrode porosity effects," *IEEE Transactions on Energy Conversion*, vol. 25, no. 3, pp. 862–872, 2010.

[4] P. Ramadass, B. Haran, R. White, and B. N. Popov, "Mathematical modeling of the capacity fade of li-ion cells," *Journal of Power Sources*, vol. 123, no. 2, pp. 230–240, 2003.

[5] L. Gao, S. Liu, and Dougal, "Dynamic lithium-ion battery model for system simulation," *IEEE Transactions on Components and Packaging Technologies*, vol. 25, no. 3, pp. 495–505, 2002.

[6] M. Chen and Rincon-Mora, "Accurate electrical battery model capable of predicting runtime and I-V performance," *IEEE Transactions on Energy Conversion*, vol. 21, no. 2, pp. 504–511, 2006.

[7] O. Erdinc, B. Vural, and M. Uzunoglu, "A dynamic lithium-ion battery model considering the effects of temperature and capacity fading," *2009 International Conference on Clean Electrical Power*, pp. 383–386, 2009.

[8] C. Binding, D. Gantenbein, B. Jansen, O. Sundstrom, P. B. Andersen, F. Marra, B. Poulsen, and C. Traeholt, "Electric vehicle fleet integration in the danish edison project - a virtual power plant on the island of bornholm," *IEEE Power & Energy Society General Meeting*, Minneapolis, MN, 25-29 Jul. 2010.

[9] H. Zhang and M.-Y. Chow, "Comprehensive dynamic battery modeling for phev applications," *IEEE Power & Energy Society General Meeting*, Minneapolis, MN, 25-29 Jul. 2010.

[10] S. Zhang, K. Xu, and T. Jow, "Electrochemical impedance study on the low temperature of li-ion batteries," *Electrochimica Acta*, vol. 49, no. 7, pp. 1057–1061, 2004.

[11] D. Haifeng, W. Xuezhe, and S. Zechang, "A new soh prediction concept for the power lithium-ion battery used on HEVs, *IEEE Vehicle Power and Propulsion Conference*, Dearborn, MI, 7-10 Sept., 2009.

[12] I. Bloom, B. Cole, J. Sohn, S. Jones, E. Polzin, V. Battaglia, G. Henriksen, C. Motloch, R. Richardson, T. Unkelhaeuser, D. Ingersoll, and H. Case, "An accelerated calendar and cycle life study of li-ion cells," *Journal of Power Sources*, vol. 101, no. 2, pp. 238–247, 2001.

[13] F. Marra, C. Træholt, E. Larsen, and Q. Wu, "Average behavior of battery-electric vehicles for distributed energy studies," *IEEE PES Innovative Smart Grid Technologies Conference Europe*, Gothenburg, 2010.

[14] O. Tremblay, L.-A. Dessaint, A.-I. Dekkiche, "A Generic Battery Model for the Dynamic Simulation of Hybrid Electric Vehicles," IEEE *Vehicle Power and Propulsion Conference* , Arlington, TX, 9-12 Sept. 2007.

[15] S. Abu-Sharkh and D. Doerffel, "Rapid test and non-linear model characterization of solid-state lithium-ion batteries", *Journal of Power Sources*, Vol. 130, no. 1-2, pp. 266-274, 3 May 2004.

[16] Bradley A. Johnson, Ralph E. White, "Characterization of commercially available lithium-ion batteries", *Journal of Power Sources*, vol. 70, no. 1, pp. 48-54, 30 Jan. 1998.

[17] J. F. Araujo Leão, L.V. Hartmann, M.B.R. Corrêa, A.M.N. Lima, "Lead-acid battery modeling and state of charge monitoring," *Applied Power Electronics Conference and Exposition (APEC), Twenty-Fifth Annual IEEE*, Palm Springs, CA, pp.239-243, 21-25 Feb. 2010.

[18] R. Rao, S. Vrudhula, D.N. Rakhmatov, "Battery modeling for energy aware system design," *Computer*, vol.36, no.12, pp. 77- 87, Dec. 2003.

[19] R. Spotnitz, "Simulation of capacity fade in lithium-ion batteries", Journal of Power Sources, vol. 113, no. 1, pp. 72-80, 1 Jan. 2003.

[i] ARPA-E – Batteries for electrical energy storage in transportation (BEEST), List of funded projects available on: http://arpa-e.energy.gov/ProgramsProjects/BEEST.aspx

